NASA/CR—2007–214724

Core Physics and Kinetics Calculations for the Fissioning Plasma Core Reactor

C. Butler and D. Albright
Institute for Scientific Research, Inc., Fairmont, West Virginia

January 2007

The NASA STI Program…in Profile

Since its founding, NASA has been dedicated to the advancement of aeronautics and space science. The NASA Scientific and Technical Information (STI) Program Office plays a key part in helping NASA maintain this important role.

The NASA STI program operates under the auspices of the Agency Chief Information Officer. It collects, organizes, provides for archiving, and disseminates NASA's STI. The NASA STI program provides access to the NASA Aeronautics and Space Database and its public interface, the NASA Technical Report Server, thus providing one of the largest collections of aeronautical and space science STI in the world. Results are published in both non-NASA channels and by NASA in the NASA STI Report Series, which includes the following report types:

- TECHNICAL PUBLICATION. Reports of completed research or a major significant phase of research that present the results of NASA programs and include extensive data or theoretical analysis. Includes compilations of significant scientific and technical data and information deemed to be of continuing reference value. NASA's counterpart of peer-reviewed formal professional papers but has less stringent limitations on manuscript length and extent of graphic presentations.

- TECHNICAL MEMORANDUM. Scientific and technical findings that are preliminary or of specialized interest, e.g., quick release reports, working papers, and bibliographies that contain minimal annotation. Does not contain extensive analysis.

- CONTRACTOR REPORT. Scientific and technical findings by NASA-sponsored contractors and grantees.

- CONFERENCE PUBLICATION. Collected papers from scientific and technical conferences, symposia, seminars, or other meetings sponsored or cosponsored by NASA.

- SPECIAL PUBLICATION. Scientific, technical, or historical information from NASA programs, projects, and missions, often concerned with subjects having substantial public interest.

- TECHNICAL TRANSLATION. English-language translations of foreign scientific and technical material pertinent to NASA's mission.

Specialized services also include creating custom thesauri, building customized databases, and organizing and publishing research results.

For more information about the NASA STI program, see the following:

- Access the NASA STI program home page at <http://www.sti.nasa.gov>

- E-mail your question via the Internet to <help@sti.nasa.gov>

- Fax your question to the NASA STI Help Desk at 301–621–0134

- Phone the NASA STI Help Desk at 301–621–0390

- Write to:
  NASA STI Help Desk
  NASA Center for AeroSpace Information
  7115 Standard Drive
  Hanover, MD 21076–1320

NASA/CR—2007–214724

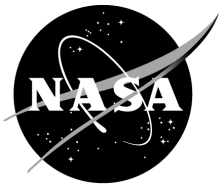

Core Physics and Kinetics Calculations for the Fissioning Plasma Core Reactor

C. Butler and D. Albright
Institute for Scientific Research, Inc., Fairmont, West Virginia

Prepared for Marshall Space Flight Center
Under Cooperative Agreement NCC8-225

National Aeronautics and
Space Administration

Marshall Space Flight Center • MSFC, Alabama 35812

January 2007

Available from:

NASA Center for AeroSpace Information
7115 Standard Drive
Hanover, MD 21076–1320
301–621–0390

This report is also available in electronic form at
<https://www2.sti.nasa.gov>

EXECUTIVE SUMMARY

NASA is developing highly efficient, compact nuclear reactors for spacecraft propulsion. Due to the high cost of testing nuclear systems, analysis and simulation present an effective method for investigating the formidable technical challenges to the development of practical nuclear space drive systems. This analysis and simulation effort has focused on the technical feasibility issues related to the nuclear design characteristics of a shockwave-driven gaseous-core nuclear propulsion system, the Fissioning Plasma Core Reactor (FPCR) as discussed in Section 1. The nuclear design of the system depends on two major calculations: core physics calculations (Section 2) and the kinetics calculations (Section 3).

The results of the previous core physics calculations were described in the ISR reports, Monte Carlo FPCR Feasibility Analysis, dated May 1, 2002 and FPCR Baseline Performance Using the MCNP4C Code, dated August 1, 2002. Presently, core physics calculations have concentrated on the use of the MCNP4C code. However, the calculation of results using alternative codes, such as the COMBINE/VENTURE codes or the SCALE4a.a code system, has begun with some initial results presented in Section 2. These alternate codes can be used for comparison with the MCNP4C results for verification and validation. These alternate codes can also be used to expand the possible scope of the calculations.

The equations and models used for kinetics calculations performed here were described in the ISR report, FPCR Kinetics Feasibility Analysis, dated May 1, 2002. Recently, several significant modifications to the ISR-developed QCALC1 kinetics analysis code have been made. These modifications include testing the state of the core materials, an improvement to the calculation of the material properties of the core, the addition of an adiabatic core temperature model and improvement of the first order reactivity correction model. The accuracy of these modifications has been verified, and the accuracy of the point-core kinetics model used by the QCALC1 code has also been validated. Previously calculated kinetics results for the FPCR were described in the ISR report, QCALC1: A Code for FPCR Kinetics Model Feasibility Analysis, dated June 1, 2002.

TABLE OF CONTENTS

TABLE OF CONTENTS (Continued)

LIST OF FIGURES

LIST OF TABLES

1 INTRODUCTION

Safe and efficient nuclear reactors using both fission and fusion techniques are prime candidates for spacecraft propulsion beyond the orbit of Mars. One of these reactor types is the Fissioning Plasma Core Reactor (FPCR)[1,2,3,4,5], which was initially conceived at the Innovative Nuclear Space Power and Propulsion Institute (INSPI) at the University of Florida.

There are many technical challenges to the development of practical nuclear space drive systems. Current nuclear technology poses significant safety concerns for spacebased missions. The testing of any nuclear system includes the high cost of test reactors and prototypes. For these reasons the use of analysis and simulation presents an effective method for investigating and addressing these issues.

Two of the key analyses for the FPCR are core physics and kinetics[6]. Issues of primary interest during the evaluation include the dimensions and shape of the core, the thickness of the reflector and the type and mass of fissile materials required. Another issue is the kinetic behavior of the core during normal operation including both subcritical and prompt supercritical conditions.

In the core physics analysis, the detailed neutron flux distribution and power distribution for the core are calculated for the core fuel and at the desired inlet temperature at different values of the core pressure. The FPCR core fuel is a tetrafluoride gas of a fissile actinide isotope such as U^{235} or Pu^{239}. The inlet temperature, T, must be high enough so that the core fuel remains a vapor throughout the cycle yet low enough so that there is no thermal damage to the vessel. The core physics analysis also yields input data for the kinetics calculation including the prompt neutron lifetime and the effective multiplication factor.

Because the FPCR is a pulsing nuclear reactor, the kinetics analysis yields the time-dependent reactor power during normal operating conditions. The power for the reactor is then used to determine the core temperature.

---

[1] NEP with Vapor Core Reactor & MHD, Travis Knight, Ph. D. University of Florida, University of Florida

[222] Multimegawatt Nuclear Electric Propulsion with Gaseous and Vapor Core Reactors with MHD, Travis Knight, Samim Anghaie, Blair Smith, Michael Houts, University of Florida

[3] Ultrahigh Temperature Vapor Reactor and Magneto Conversion for Multi-megawatt Space Power Generation, Nils J. Diaz, Samin Anghaie, Edward T. Dugan & Isaac Maya, Space Power Vol 8, Nos. ½ 1989, University of Florida

[4] Overview of Nuclear MHD Power Conversion for Multi-Megawatt Electric Propulsion, Blair M. Smith, Travis W. Knight, Samin Anghaie, Innovative Nuclear Space Power and Propulsion and University of Florida

[5] Ultrahigh Temperature Vapor-Core Reactor-Magnetohydrynamic System for Space Nuclear Electric Power, Isaac Maya, Samin Anghaie, Nils Diaz and Edward T. Dugan, Journal of Propulsion and Power, Vol 9, Jan-Feb 1993, University of Florida

[6] Functional Requirements for the Evaluation of a FPCR Propulsion System, Institute for Software Research, October 5, 2001

1.1 Model Overview

A simplified block diagram of the FPCR system is shown in Figure 1-1. The design of the core and the systems in the immediate vicinity of the core are shown in Figure 1-2. The geometry of the core/reflector system is shown in Figure 1-3.

The vapor in the core consists of a 100% enriched fissile Actinide, like U^{235} or Pu^{239}, in a tetrafluoride form either UF_4 or PuF_4. Overlapping shock waves compress[7] the vapor in the core, inducing nuclear criticality. This is because the compression of the vapor increases the vapor density thereby increasing the macroscopic fission cross-section. The increase in the macroscopic fission cross-section increases the effective multiplication factor. The FPCR pulses when the effective multiplication factor exceeds 1, then the power in the reactor increases very rapidly to a design level in the megawatt range.

The power pulse amplitude decreases when the shock wave passes the vapor resulting in vapor decompression and, therefore, a reduction in the macroscopic cross-sections. This in turn results in a decrease of the effective multiplication factor. When the reactor is subcritical, the effective multiplication factor is less than 1; then the core power decreases very rapidly to a very low level.

[7] S. Anghaie and H. Dai, "Shockwave Phenomena and High Pulsed Magnetic Field', Internal Report, Innovative Nuclear Space Power and Propulsion Institute, University of Florida

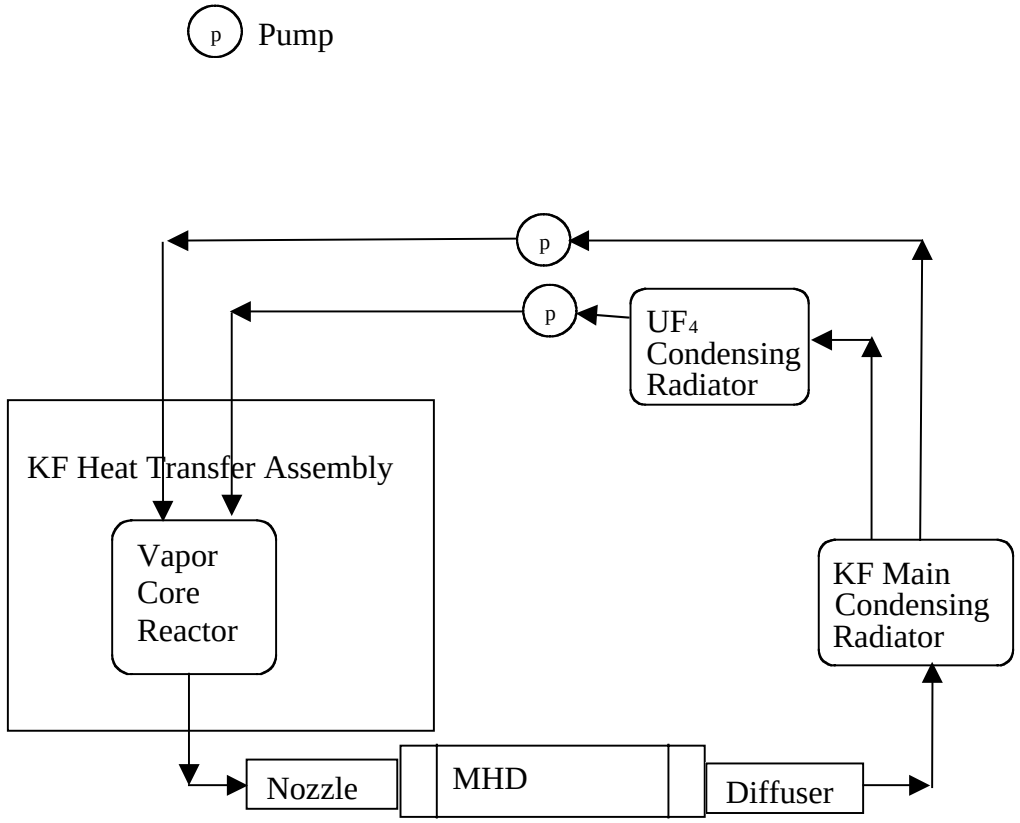

Figure 1-1. FPCR Simplified System Block Diagram[8]

[8] Ultrahigh Temperature Vapor-Core Reactor-Magnetohydrodynamic System for Space Nuclear Reactors-Magnethydrodynamic System for Space Power, Isaac Maya, Samin Anghaie, Nils J. Diaz, Edward T. Dugan, Journal of Propulsion and Power, Vol 9, Jan-Feb 1993, University of Florida

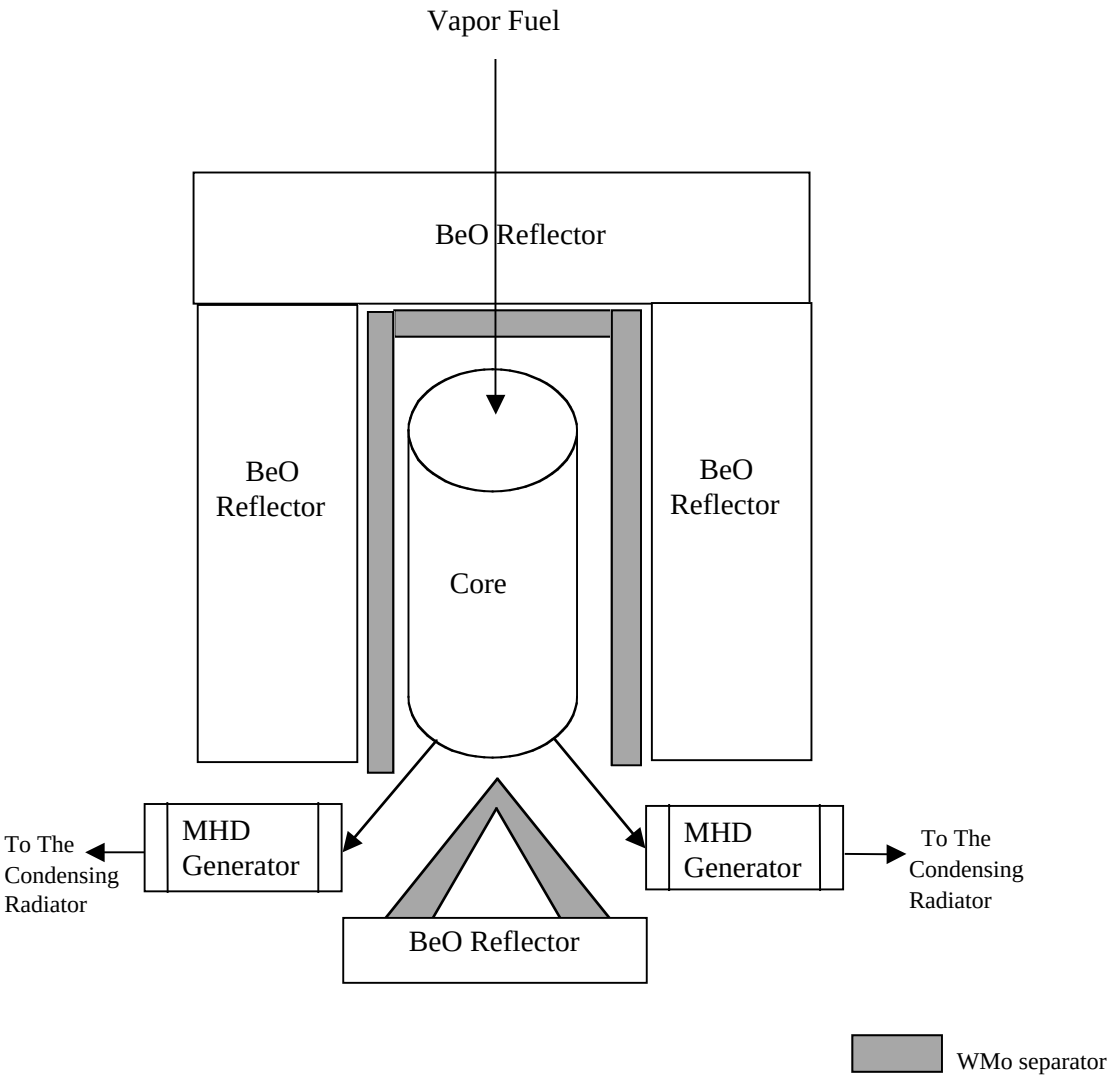

Figure 1-2. FPCR Simplified Core Diagram

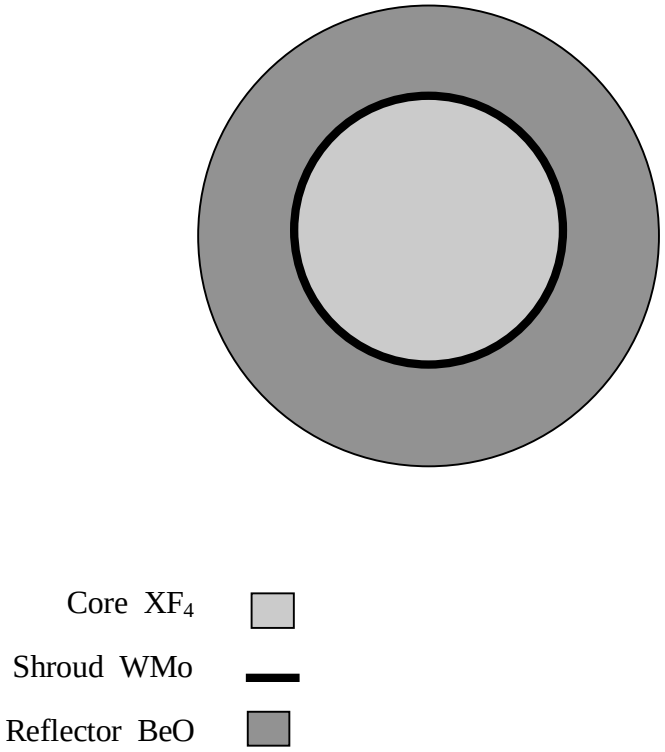

Figure 1-3. FPCR Simplified Core/Reflector Geometry

1.2 Purpose of the Calculations

The analyses performed at the Institute for Scientific Research determined the nuclear properties of the FPCR. These nuclear properties include the core power distribution, the effective multiplication factor and the dynamic properties of the power pulse of the FPCR. These nuclear properties have been obtained for a large number of fissile isotopes as well as for a moderate number of inlet temperatures and can help to determine which fissile isotopes should be used in the final core design.

1.3 Preliminary Description of the Calculations

The calculations performed at ISR consist of two parts, a core physics calculation and a kinetics calculation. The core physics calculations are presently used to provide input data to the kinetics code. The kinetics code uses this input data to determine the detailed dynamic behavior of the power in the core.

More than one core physics code system must be used to obtain accurate core physics calculations. A set of codes will usually consist of a cross-section library, a material physics code, a core physics code and possibly a number of codes. The basic components of a code system are illustrated in Figure 1-4. The symbols used in this figure are further explained in Figure 1-5. The cross-section library contains neutron cross-sections for many different isotopes and materials that depend explicitly upon the neutron energy. The material physics code uses the core compositional data and a very simplified core geometry to calculate the macroscopic cross-sections for use by the core physics code. The core physics code calculates almost all of the important results used. The miscellaneous codes are used to interpret the core physics results, do some relatively simple calculations, generate graphics and, in general, make the core physics results more easily understood. The kinetics code is used to determine the time dependence of the power level of the reactor.

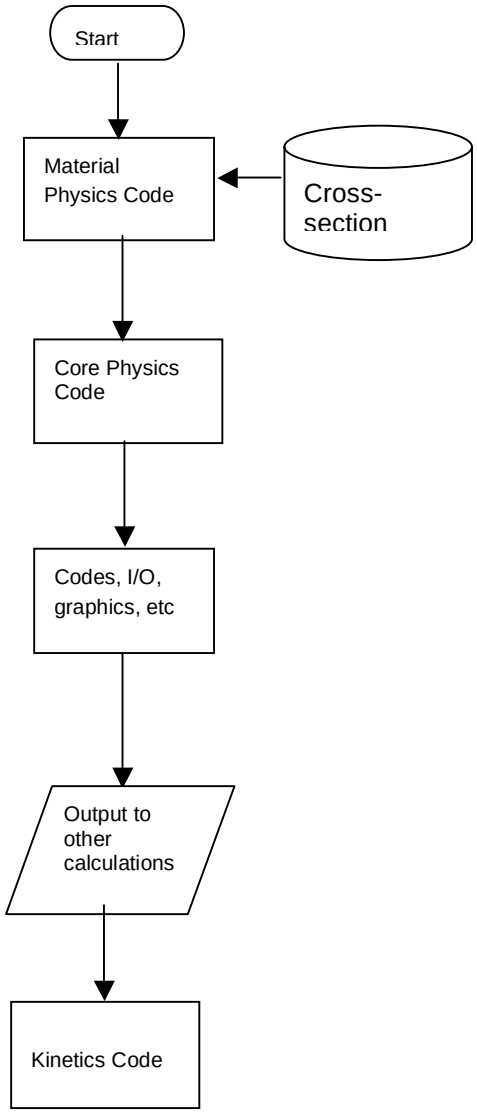

Figure 1-4. Basic Components of a Code System

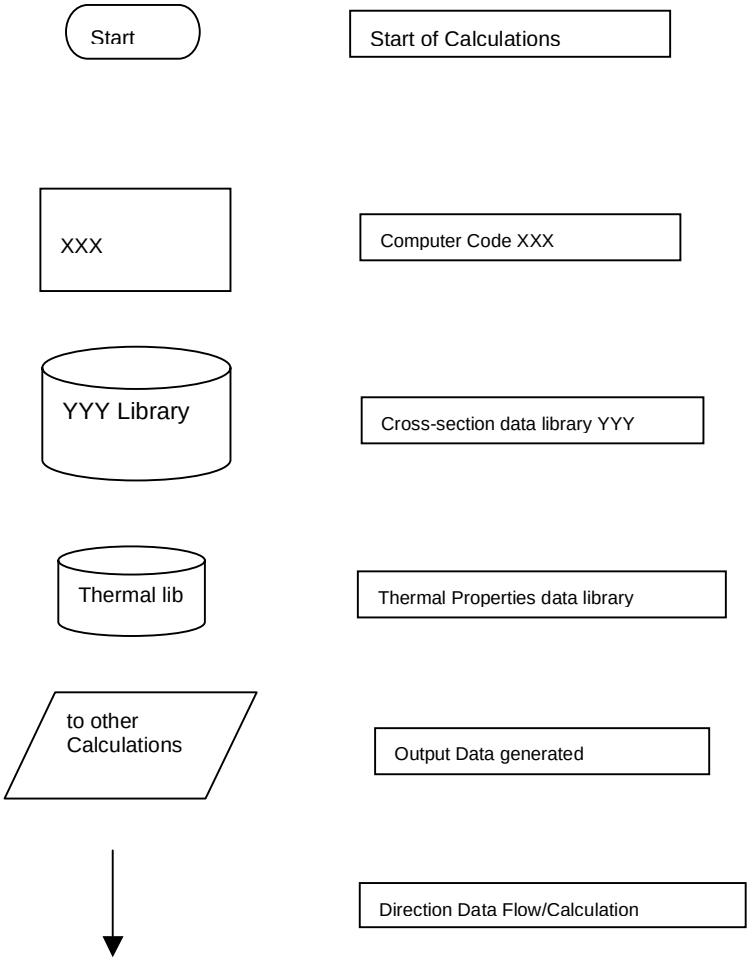

Figure 1-5. Code System Legend

1.4 Using Multiple Code Systems

Comparing core physics results with experimental data or plant data is called benchmarking. There may be small biases in each of the codes available, as well as a number of biases in how the input data is prepared. If there is little or no experimental data, the only alternative is an inter-code comparison. No reactors exist that are similar enough to the FPCR both in materials and operational conditions to facilitate benchmarking. For this reason it is necessary to use multiple core physics codes systems to perform detailed inter-code system comparison.

Even if there is experimental data or plant data, it may be very useful to compare the data with the results calculated by a number of code systems. This is because different code systems are based on different modeling assumptions. Using different code sets may be useful in determining which of these sets of assumptions are valid and therefore which code set should be used for future calculations.

Another reason for the use of multiple codes is that each of the code systems may have capabilities that other code systems do not. Some calculations may be much more easily done by one code system than by another, or one code system may have an output format that is more complete or more easily interpreted than the other code system.

For all of these reasons two additional code systems, COMBINE/VENTURE and SCALE4a.a were used to supplement the MCNP4C code to model the FPCR. The DOORS3.2 code system, based on neutron transport theory, was considered for the calculation but is presently unavailable.

2 CORE PHYSICS CALCULATIONS

Multiple code systems were used to perform the core physics calculations for FPCR. Each of these code systems and their utilization is described in below.

2.1 Use of the MCNP4C Code

The MCNP4C code system has been successfully installed and a large number of cases have been run successfully, as described in a previous report[9]. This section provides a short description of the MCNP4C code system, a description of the model used for FPCR, and for the recently obtained results.

2.1.1 Description of the MCNP4C Code System

The components of the MCNP4C[10] code system are shown in Figure 2-1. In the MCNP4C code system, no materials physics calculation is needed because the MCNP4C code obtains the required cross-sections from the ENDF-B5[11] cross-section library. The ENDF-B5 cross-section library contains data for 66 neutron energy groups and all of the required isotopes. It is the standard neutron cross-section library used throughout the industry.

The MCNP4C code is a multi-group Monte Carlo code capable of accurately modeling any reactor system including the FPCR. It also has the capability to model eigenvalues and the effective multiplication factor. MCNP4C requires relatively detailed geometric and compositional data for input data. Point-wise cross-section data are used where all reactions in a given cross-section evaluation are implemented.

The MCNP4C code has three different sources and both geometry, output tally plotters and a flexible tally structure making the output of the MCNP4C code user-friendly. Because of the flexibility added by these user-friendly features, and the fact that MCNP4C is a Monte Carlo code, it is able to perform virtually all of the types of calculations required. Despite the inherent accuracy of the MCNP4C code some benchmarking data must be provided either from experimental results or by other core physics code systems. This data is necessary to either enhance or verify the accuracy of the core physics calculation performed with the MCNP4C code system.

[9] Monte Carlo FPCR Feasibility Analysis, MAP-2002-V-F024-UNCLASS-050102, May 1, 2002
[10] RSICC Computer Code Collection. MCNP-1 A General Monte Carlo N-Particle Transport Code Version 4C, LA-13709-M, Los Alamos National Laboratory, April 2000.
[11] B. A. Magurno, et al., Guidebook for the ENDF/B-V Nuclear Design Files, EPRI NP-2150, July 1982

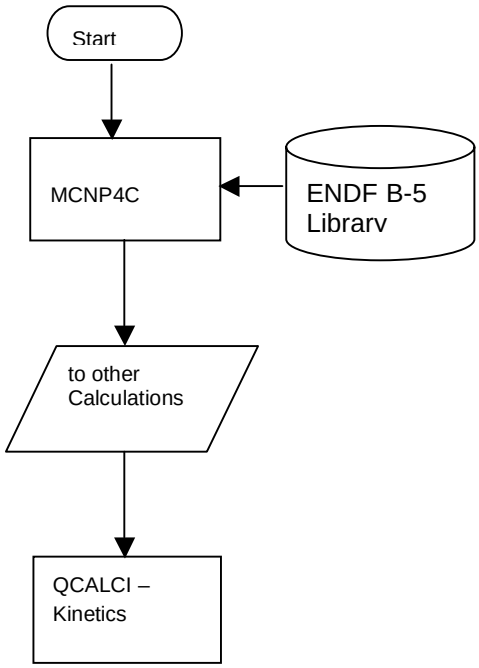

Figure 2-1. Components of the MCNP4C Code System

2.1.2 Calculations with the MCNP4C Code

The MCNP4C baseline, created to approximate criticality of the FPCR, was developed in two stages. First, a series of static parametric analyses was conducted to model criticality behavior as a function of fuel composition, temperature, reflector thickness and separator thickness. Then using the information gained from the static parametric analyses a dynamic infinite multiplication factor, k_∞, model was developed to better simulate the reactor during compression.

The static parametric study was conducted to analyze how the fuel composition, temperature, reflector thickness and separator thickness affected criticality of the FPCR as a function of pressure. The parametric study is referred to as the static model because the volume of the core remained fixed at $3m^3$. For each parametric test, 12 different pressures were used to describe how the criticality of the system behaved while the pressure is increased from .5 MPa to 50 MPa. For each static case a single value of the effective multiplication factor, k_{eff}, was obtained and was used to establish a system baseline for the FPCR. From the static parametric analyses, it was found that

1) the core design of the FPCR concept was feasible

2) the fissile isotopes, U^{235} and Pu^{239}, were acceptable candidates for fuel. Other candidate isotopes and mixtures of isotopes were also modeled and are still possible candidates for fuel.

Upon conclusion of the static parametric analyses, a dynamic model for the infinite multiplication factor, k_∞, was developed to determine the number of nodes needed to describe the neutronics of the FPCR reactor system. The number of nodes needed to describe accurately the neutronics of a system can be determined by analyzing the system's criticality values as functions of the number and location of nodes.

To determine axial uniformity, a localized criticality value, the infinite multiplication factor, k_∞, was computed as a function of position for Pu^{239} and the U^{233}-U^{235} mixture noted in the parametric analyses summary. Likewise, the criticality behavior of the reactor system was tested for radial uniformity.

To determine the radial behavior of the core, the infinite multiplication factor, k_∞, was computed for the selected fuels as a function of the radial distance from the axis of the core at 1) the core center and 2) at the two core boundaries adjacent to the reflectors. The FPCR was evaluated using MCNP4C to establish a system baseline[12]. From this dynamic analysis, it was found that a point kinetics analysis is adequate to evaluate the properties of the FPCR core.

[12] Monte Carlo FPCR Feasibility Analysis In Progress Report, Institute for Software Research, Fairmont, West Virginia, May 1, 2002.

2.2 Use of the COMBINE/VENTURE Code System

The COMBINE/VENTURE code system has been successfully installed and all of the test cases have been run successfully. This subsection provides a short description of the COMBINE/VENTURE code system and a description of the status of the models for two codes.

2.2.1 Description of the COMBINE/VENTURE Code System

The components of the COMBINE/VENTURE code system are shown in Figure 2-2.

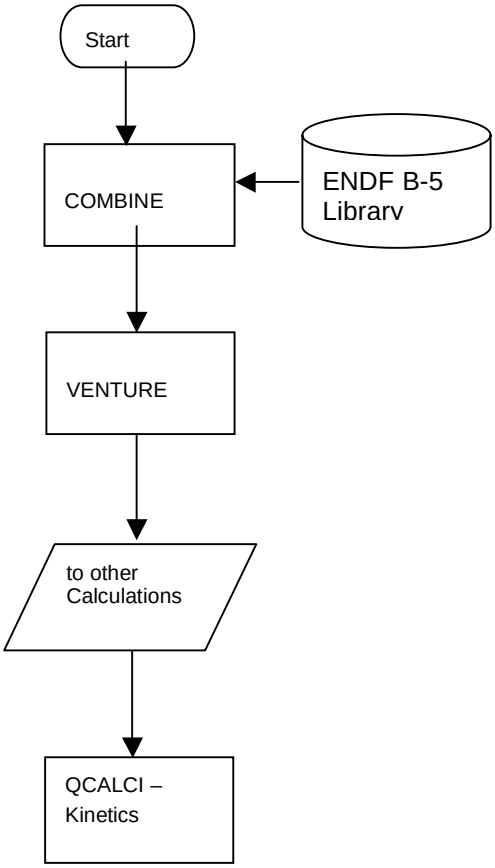

Figure 2-2. Components of the COMBINE/VENTURE Code System

The neutron cross-section library used by the COMBINE/VENTURE code system is the ENDF-B5 cross-section library. The ENDF-B5 cross-section library contains data for 66 neutron energy groups and all of the isotopes required; it is the standard neutron cross-section library throughout the industry.

In the COMBINE/VENTURE code system, the materials physics calculation used the COMBINE code. The COMBINE[13,14] code is an advanced neutron transport theory code using multiple neutron energy groups and the B-3 approximation, where the geometry of the core is modeled very crudely while multi-group macroscopic cross-sections are calculated in a very accurate manner.

The COMBINE code calculates the fast neutron spectrum, solves the neutron thermalization problem, solves for the thermal neutron flux and averages the cross-sections. The fast neutron spectrum is calculated using a Dancoff-Ginsburg correction factor with a resonance absorption calculation. The COMBINE code solves the neutron thermalization problem by calculating energy dependent neutron spectra and averages the cross-sections to generate multi-group cross-sections. The COMBINE code can use a B-1 spherical harmonic approximation solved using a Gauss-Seidel iterative scheme. The COMBINE code obtains the required average cross-sections, which are then calculated using neutron slowing theory and energy dependent cross-section data.

The VENTURE[15] code obtains macroscopic cross-section data from the COMBINE calculations. The VENTURE code uses multiple neutron energy groups. In the VENTURE code, finite difference techniques are used to solve either the neutron diffusion equation or the P1 neutron transport equation. The VENTURE code uses an inner-outer iteration scheme with an over-relaxation scheme to obtain the neutron fluxes. The VENTURE code solves the coupled burn-up differential equations and then explicitly solves for the resulting coupled nuclide chains.

The VENTURE code is capable of accurately modeling any reactor system, including the FPCR. Like most other diffusion theory codes, the VENTURE code is relatively flexible and is able to perform most, if not all, of the calculations required; it can, therefore, be used for multiple types of production and design calculations.

The COMBINE and VENTURE codes, have relatively simple input data requirements and are very compatible with each other. However, for extremely accurate calculations, boundary condition data must be provided by other codes, like MCNP4C, or the SCALE4.4a code system.

[13] COMBINE/PC-Code System to Compute Neutron Spectra and ENDF/B Version 5 Based Multigroup Neutron Constants, EG&G Idaho Inc., August 1991
[14] Robert A. Grimsey, David W. Nigg, Richard L. Curtis, COMBINE/PC-A Portable ENDF/B Version 5 Neutron Spectrum and Cross-Section Generation Program, EG&G Idaho Inc., April 1990
[15] A. Shapiro, H. C. Huria, K. W. Cho, VENTURE/PC MANUAL A Multidimensional Multi-group Neutron Diffusion Code Version 2 , University of Cincinnati, January 1990

2.2.2 Use of the COMBINE Code

Input data for the COMBINE calculation consists of the exact isotopic composition data for the core medium consisting of the number densities of the isotopes or elements in the core. The range of pressures and temperatures of the core medium during operating conditions are necessary for this calculation. The SIZE1 code was modified to produce both temperature-dependent and pressure-dependent input data for the COMBINE code. Because of this modification, the number densities for all materials in the core were calculated for a very wide range of both pressures and temperatures by the SIZE1 code. The SIZE1 code is further described in the third section of this report.

The modeling process for the COMBINE code for the Fissioning Plasma Core Reactor, FPCR, was started. However, difficulties arose because the FPCR is a gas core reactor with a reflector, and the fissile materials have low densities. Proper incorporation of the effect of the reflector in the fuel cross-sections with very low densities difficult. The slowing-down effect of the reflector should affect the cross-sections of the fuel but the cross-sections of the reflector should not be added to those of the fuel. The initial pressures of the gas resulted in very low number densities of the fuel, near the lower limit of the number densities allowed by the COMBINE code.

Despite these difficulties, a series of calculations were performed modeling the core with neither the shroud nor the reflector. These calculations were done throughout the pressure operating range of the FPCR (.5 MPa $\leq p \leq$ 50.0 Mpa) for two different core temperatures, 2000 K and 3000 K, and the two most important fissile isotopes, U^{235} and Pu^{239}. The element Fluorine, F, was also included in the composition of the core.

The results of these calculations shown in Figure 2-3, are as expected. For all isotopes and core temperatures, the infinite multiplication factor is a maximum at low pressures; it then gradually decreases as the pressure is increased. This is an expected result because the infinite multiplication factor, k_{inf}, is approximately proportional to the number of neutrons per fission, ν. The number of neutrons per fission, ν, is a slowly increasing function of the average neutron energy. The average neutron energy will decrease as the pressure increases because number density increases, increasing the moderation.

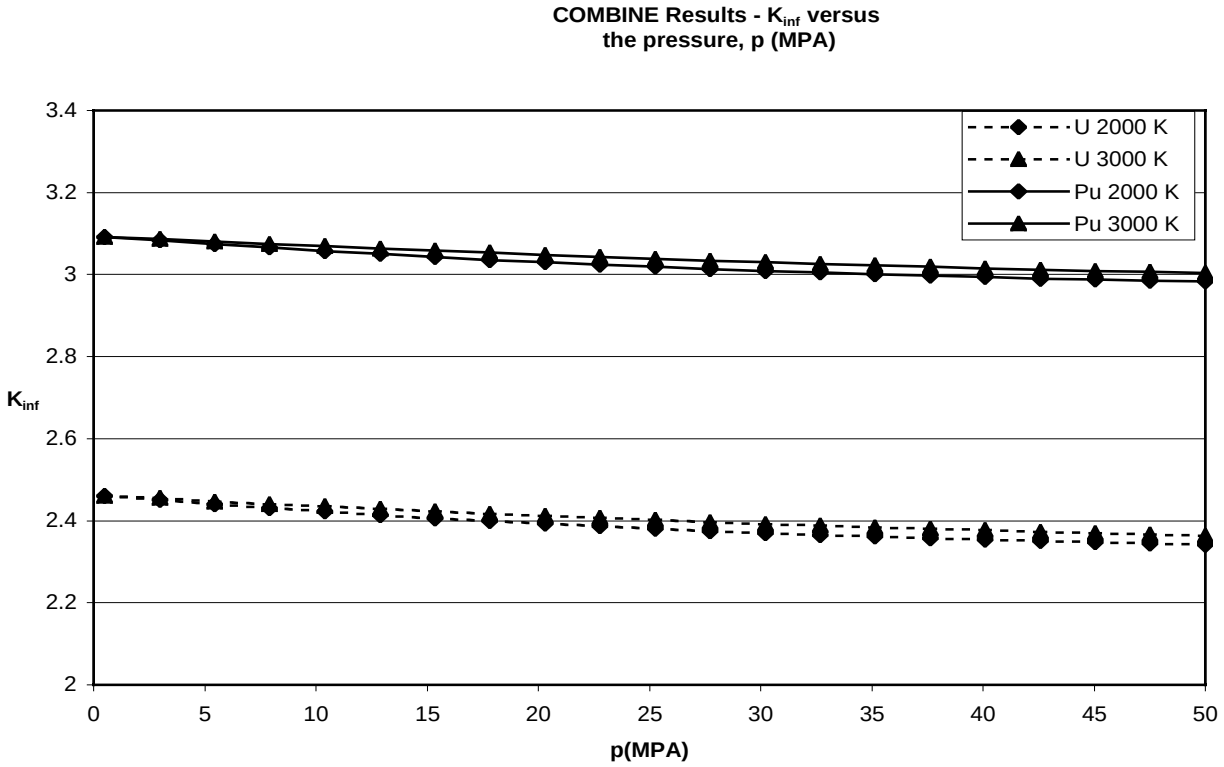

Figure 2-3. COMBINE Results – Infinite Multiplication Factor, k_{inf}, vs pressure, p

2.2.3 Use of VENTURE Code

As stated in the 2002 Marshall Advanced Propulsion Statement of Work, confidence in the prediction of system operation is reinforced by the use of a number of different core physics codes such as the diffusion theory code system, COMBINE/VENTURE, and the Monte Carlo code, MCNP4C, where the predictions are all in close agreement. A comparison of the predictions generated by the COMBINE/VENTURE code system against the results of the FPCR MCNP4C baseline results would be a good indicator of the accuracy of the FPCR model based upon given parameters.

The VENTURE/COMBINE code system poses several challenges. One of the challenges posed by the code packages include the inability to properly define material cross-sections at the necessary temperatures. This is due to the present code features and the inadequacies of the user's manuals. However, a basic understanding of the VENTURE input modules has been achieved.

Three input card modules were identified as the basic modules, both necessary and available, to simulate the core physics of the FPCR using the VENTURE/COMBINE code system. These three basic modules are the control module, the input processor module, and the special processor modules. The relationship between these modules is shown in Figure 2-4. These three basic modules must always be included in a VENTURE input card.

The first module to be entered is the control module. The control module initiates the code, contains the file name and specifies the necessary amount of memory allocation.

The second module that appears on a VENTURE input card is the input processor module. The input processor module defines the material cross-section data that VENTURE will use to calculate the user's desired information. The material cross-sections for the fuel and reflector material at the specified pressure and temperature values must be defined to calculate the effective multiplication factor for the FPCR. The input processor module also identifies the form of the cross-sectional data. Furthermore, the input processor module allows control of the output file production.

The third module needed to simulate the core physics of the FPCR is the special processor module. Part of the third module is the DCRSPR module which produces input data for the cross-section processor module. A primary function of this module is to convert the nuclide-ordered cross-section sets in an ISOTX (isothermal cross-section data) file to a group ordered GRUPXS file as required.

The special processor DVENTR is the main module of the system. In the DVENTR module the user selects the basic particle transport methodology, indicates the tallies to be printed, defines the geometry of the reactor, and assigns nuclides to their specific geometric zones. DVENTR module provides the interface files for the neutronics module VENTURE.

A number of other modules may be used to perform core physics calculations. For example, the GRUPXS module generates group ordered microscopic cross-sections. The NDXSRF module stores the nuclide-to-cross-section referencing data. The ZNATDN module defines the nuclide atomic densities in each of the geometric zones.

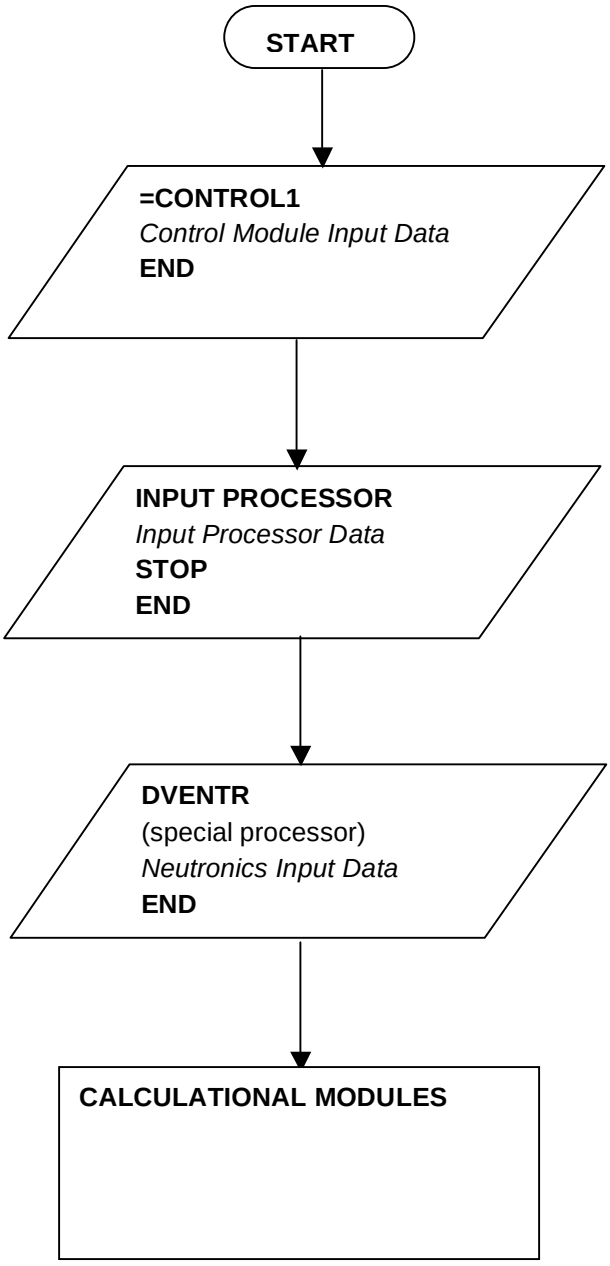

Figure 2-4. Relationship between VENTURE Input Modules

2.3 Use of the SCALE4a.a Code System

The SCALE4a.a code system has been successfully installed and the test cases were run successfully.

The SCALE4a.a code system can be used to validate the results obtained using the MCNP4C code. Furthermore, it will be demonstrated that the SCALE4a.a code system can perform a wider range of calculations than either the MCNP4C[16] code system or the COMBINE/VENTURE code.

The following subsections provide a short description of the SCALE4a.a code system and a description of the status of the models for the two most important codes, CSPAN and KENO.

2.3.1 Description of the SCALE4a.a Code System

The components of the SCALE4a.a code system are shown in Figure 2-5.

Several different neutron cross-section libraries can be used by the SCALE4a.a code system. The major difference between these cross-section libraries is the number of isotopes available and the number of neutron energy groups. The ENDF-B5 cross-section library contains data for 66 neutron energy groups and all of the isotopes required. Furthermore, this ENDF-B5 cross-section library is the standard neutron cross-section library throughout the industry. There is also available an ENDF-B5 library with 238 groups, an ENDF-B6 library with 218 groups and a Hansen-Roach library with 16 neutron energy groups but more isotopes.

In the SCALE4a.a code system, the materials physics calculation is done using the CSPAN[17] code and the XSDRNPM[18] code. The CSPAN code consists of an advanced graphical user interface (GUI) and several modules. The first of these modules, MIPLIB, allows the use of simple keywords to specify case materials and prepares input for the other modules. The BONAMI module performs the resonance shielding calculation and produces a case-dependent library of cross-sections. The NITWAL module performs the processing of the neutron cross-sections in the resonance energy group calculation using a fine energy group calculation of the slowing-down flux, weighting the flux at each resonance. The NITWAL module also produces a case-dependent master library of cross-sections. The NITWAL module can be used to convert the format of the master libraries to that of problem dependent libraries. The XSDRNPM code is a 1-dimensional neutron transport theory code used to cell-average cross-sections.

[16] RSICC Computer Code Collection, MCNP-1 A General Monte Carlo N-Particle Transport Code Version 4C, LA-13709-M, Los Alamos National Laboratory, April 2000.
[17] R. D. Busuch, S. M. Bowman, KENO V.a Primer: A Primer for Criticality Calculations with SCALE/KENO V.a Using CSPAN for Input, ORNL/TM 2002/155, August 15, 2002
[18] N. M. Greene, L. M. Petrie, XSDRNPM: A ONE DIMENSIONAL DISCRETE ORDINATES CODES FOR TRANSPORT ANALYSIS, ORNL/NUREG/CSD-2/V2/R6, March 2000

The KENO-VI[19,20] code obtains macroscopic cross-section data from the CSPAN code. The KENO-VI code is an advanced Monte Carlo code capable of accurately modeling any critical configuration or reactor system including the FPCR. The KENO-VI code uses a collision treatment based upon a Legendre expansion of the cross-section array and a Guassian quadrature procedure to generate probabilities and angles. The KENO-VI code uses weighted tracking that models neutron absorption by decreasing the weight of the neutron history, rather than eliminating it. Very low weight neutron histories are eliminated using random numbers. A differential albedo technique is used to simplify the detailed modeling of reflector regions. The KENO-VI code allows the user to model extremely complex geometry. A large number of predefined shapes as well as any geometric shape describable by quadratic equations can be used by the KENO-VI model.

Because the KENO-VI code is a Monte Carlo code that allows for the use of extremely complex geometry, it is extremely flexible and is able to perform all of the calculations required for the FPCR. However, the KENO-VI code may require relatively long running times.

The SCALE4.4a code system can do several different types of calculations. This is because it has a relatively large number of miscellaneous codes. The interpretation of the output of the KENO-VI calculation is facilitated by the PICTURE[21] code, which is a two-dimensional plotting program.

Three available heat transfer codes use the output of the KENO-VI code. The HEATING[22] code performs 3-dimensional heat transfer calculations for general geometries using the Thermal Properties library. The HTAS1[23] code uses the thermal properties library and together with the OCULAR[24] code, perform heat transfer for fuel shipping casks. The ORIGEN-S[25] code can supplement the core physics calculations of KENO-VI in many ways, including fuel depletion studies.

Since this report is primarily concerned with material physics and core physics, only the CSPAN codes and the KENO-VI code will be discussed further in any detail.

[19] L. M. Petrie, N. F Landers, KENO V.a AN IMPROVED MONTE CARLO CRITICALITY PROGRAM WITH SUPERGROUPING, ORNL/NUREG/CSD-2/R6, March 2000
[20] D. F. Hollenbach, L. M. Petrie, N. F. Landers, KENO-VI: A GENERAL QUADRATIC VERSION OF THE KENO PROGRAM, ORNL/NUREG/CSD-2/V2/R6, March 2000
[21] Margaret B. Emmet, PICTURE: A 2-D PLOTTING PROGRAM FOR MARS GEOMETRIES, ORNL/NUREG/CSD-2/V3/R6, March 2000
[22] K. W. Childs, HEATING 7.2 USER'S MANUAL, ORNL/NUREG/CSD-2/V2/R6, March 2000
[23] G. E. Giles, HTAS1: A TWO-DIMENSIONAL HEAT TRANSFER ANALYSIS OF FUEL CASKS, ORNL/NUREG/CSD-2/V1/R6, March 2000
[24] C. B. Bryan, G. E. Giles, OCULAR:A RADIATION EXCHANGE FACTOR COMPUTER PROGRAM, ORNL/NUREG/CSD-2/V2/R6
[25] O. W. Hermann, R. M. Westfall, ORIGEN-S: SCALE SYSTEM MODULE TO CALCULATE FUEL DEPLETION, ACTINIDE TRANSMUTATION, FISSION PRODUCT BUILDUP AND DECAY, AND ASSOCIATED RADIATION SOURCE TERMS, ORNL/NUREG/CSD-2/V2/R6, March 2000

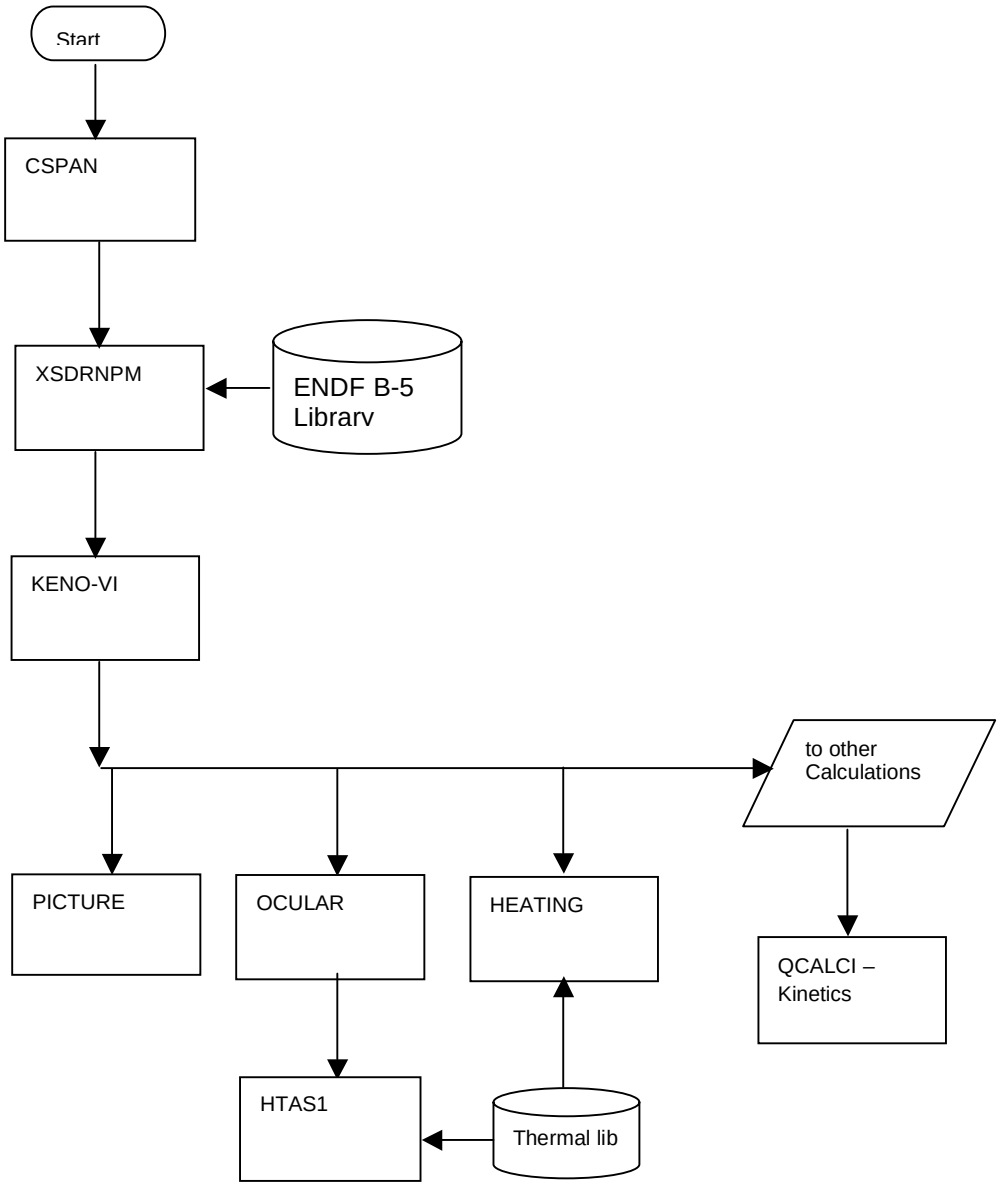

Figure 2-5. Components of the SCALE4a.a Code System

2.3.2 Use of the CSPAN Code

Due to time constraints, only familiarization was performed with the material physics code, CSPAN. Although no successful calculations were performed with these two codes, the SIZE1 code was modified to produce both temperature and pressure dependent input data for the CSPAN code. This will greatly facilitate preparation of input data when the results of numerous material physics calculations are required at different pressures and temperatures.

2.3.3 Use of the KENO-VI Code

Simulation efforts were focused upon the development of a working FPCR model using a criticality control module found in the code package SCALE4.4a. In August, ISR and MSFC agreed to validate criticality predictions generated by the criticality control module, KENO-VI, against the MCNP4C baseline. Although, KENO-VI and MCNP4C both use Monte Carlo techniques to calculate k_{eff}, the two codes are independent. In the nuclear industry, the KENO code is very commonly used to validate MCNP results. Therefore, confidence in the prediction of system operation will be reinforced if the FPCR model predictions using KENO-VI are in close agreement with the results of MCNP4C calculations.

The sample problem for the KENO-VI code was run successfully. The results were validated by comparison with the output files supplied with the SCALE4a.a system. There was excellent agreement between the two sets of output indicating that the KENO-VI code had been properly installed at ISR.

Currently, a series of KENO-VI input cards are being developed to compare against the MCNP4C baseline. This set of KENO-VI input cards, k15b1 – k15b12, have the same parameters as the the15b series of MCNP4C input cards, 15b1-15b12. The parameters are as follows:

BeO reflector thickness= 20 cm,

MoW separator thickness= 1 cm

The temperature of the core (T_c) is fixed at 1500 K

The temperature of the reflector (T_r) and separator (T_s) are fixed at 300 K.

As implemented in the MCNP4C parametric test series, the k15b KENO-VI input series are composed of twelve input cards with pressure increasing from 0.5 MPa to 1.0 MPa, 1.0 MPa to 5.0 MPa, then from 5 MPa to 50 MPa in intervals of 5 MPa. Development of the KENO-VI input cards is presently ongoing. Key code features, such as material definition, need to be researched further before the KENO-VI input cards fully represent the input data used during formation of the MCNP4C baseline.

2.3.4 Use of the SCALE4a.a Miscellaneous Codes

Since a complete set of KENO-VI input data set is not presently available, the preparation of input data for any of the miscellaneous codes of the SCALE4a.a code system has not been started.

3 IMPROVEMENTS TO THE QCALC1 KINETICS CODE

The kinetics modeling of the FPCR is done by the QCALC1 code. A previous version[26,27] of the QCALC1 code has been described. This section documents the recently implemented modifications to the QCALC1 code and a validation study recently applied to the QCALC1 code. Future modifications are also suggested.

The QCALC1 code has had its validity tested to ascertain the accuracy of the point-core model. This has not yet been documented in a report.

Three modifications were performed: improvement of the core thermal properties in the model, including the testing of the state of the fluid, an improved core temperature model, and the addition of improved temperature/density reactivity correction models. The validation, the three types of modifications, and possible future modeling enhancements and improvements are described below.

[26] FPCR Kinetics Feasibility Analysis In Progress Report, MAP-2002-V-F025-UNCLASS-050102, May 1, 2002

[27] QCALC1: A Code for FPCR Kinetics Model Feasibility Analysis , MAP-2002-V-UNCLASS-060102, June 1, 2002

3.1 Accuracy of the Point-core Model

In kinetics, a point-core model approximates the core as a single node. The point-core model is usually the standard model for kinetics calculation and therefore is used rather than other nodalizations if its accuracy has been validated. A point-core model is accurate if the distance the average neutron travels before capture is more than any dimension of the core. However, if the distance the average neutron travels before capture is significantly smaller than a dimension of the core, a multi-node model must be used.

For simplicity, the QCALC1 code uses a point-core model for the kinetics. To prove the accuracy of the point-core model, the diffusion length, L, which is essentially the relaxation length for the flux, must be calculated. Then the diffusion length must be compared with the dimensions of the core, the core height, h, and the core radius, R.

The SIZE1 code varies the temperature and pressure over a wide range; it uses microscopic cross-section data and isotopic data to calculate the diffusion length. The SIZE1 code also calculates a number of input quantities for the material physics codes, including the number density for the COMBINE code, and the density for the CSPAN code. These calculations greatly facilitate the development of input data for both COMBINE and CSPAN. The SIZE1 code was also used to develop many of the models described later in this section.

The figures in this subsection show the dependence of diffusion length, L, for the tetra fluoride of a fissionable isotope, as functions of the pressure, p, for a range of core inlet temperatures, T. The range of pressures shown in the figures is that to be used in the FPCR. The core height, h, and the core radius, R, are also shown in these figures.

Using an isothermal temperature model, we have found that the diffusion length is initially larger than the core height for all fissile isotopes, all neutron energies, E, and all core temperatures, T, studied. With increasing pressure the core height very rapidly decreases; the diffusion length also decreases, but less rapidly than the core height. For all pressures used in the FPCR, as well as for all fissile isotopes, all neutron energies, E, and all core temperatures, T, shown, the diffusion length, L, is much larger than the core height:

$$L > h$$

With respect to the core height, h, these figures strongly suggest that a point-core nodalization is an adequate approximation for the kinetics model.

The diffusion length is initially much larger than the core radius, R, for all fissile isotopes, all neutron energies, E, and all core temperatures, T, studied. However, in the present model of the core, including the use of the isothermal temperature model, the core radius is assumed to remain constant. Since the diffusion length decreases, it may be smaller than the core radius for a range of relatively high pressures and low temperatures:

$$p \geq p_{\max 1}$$

$$T \leq T_{\min 1}$$

$$L < R$$

This suggests that a point-core nodalization for the kinetics model may not be accurate for these low inlet temperatures and in this pressure range if the isothermal temperature model is used. However, the diffusion length increases relatively rapidly with the core temperature and may be larger than the core radius for a large range of pressures:

$$T > T_{\min 1}$$

$$L > R$$

Therefore, the point-core model is accurate for virtually all pressures and sufficiently high core temperatures if the isothermal model is used. This is shown in Figure 3-1 for U^{235} and in Figure 3-2 for Pu^{239}.

The value of the temperature is shown in the legend of the figures. The isothermal temperature model, which is further described in Subsection 3.3.2, is probably a poor approximation. The core temperature, T, is modeled using the isothermal temperature model in the QCALC1 code as:

$$T = T_0 + \Delta T(q)$$

where T_0 is the inlet temperature and $\Delta T(q)$ is the temperature rise due to the heat generated by fission. The maximum value of $\Delta T(q)$ is approximately $1000^{o}K$ for every megawatt of power, q. Using the adiabatic temperature model, the core temperature will increase rapidly with increasing pressure, p:

$$T = T_A(p) + \Delta T(q)$$

where $T_A(p)$ represents the adiabatic temperature model, described in detail in Subsection 3.3.1. A comparison between the adiabatic temperature model and isothermal temperature model is shown in Figure 3-6. The adiabatic temperature model calculates the core temperature based upon the compression of the gas from the initial conditions of pressure, p_0, volume, V_0, and the inlet temperature, T_0, to the state with pressure, p. The adiabatic temperature model, T_A, will increase the core temperature from 2000 K to over 4000 K while the pressure increases from .5 MPa to 50.0 MPa. The increased core temperature substantially increases the diffusion length so that it will exceed the core radius, making a point-core kinetic model an excellent approximation. This is shown in Figure 3-3 for U^{235} and in Figure 3-4 for Pu^{239} where the diffusion length, L, is always greater than both important core dimensions:

$$L > h$$

$$L > R$$

Therefore, the point-core model is accurate for virtually all pressures and inlet temperatures if the adiabatic temperature model is used.

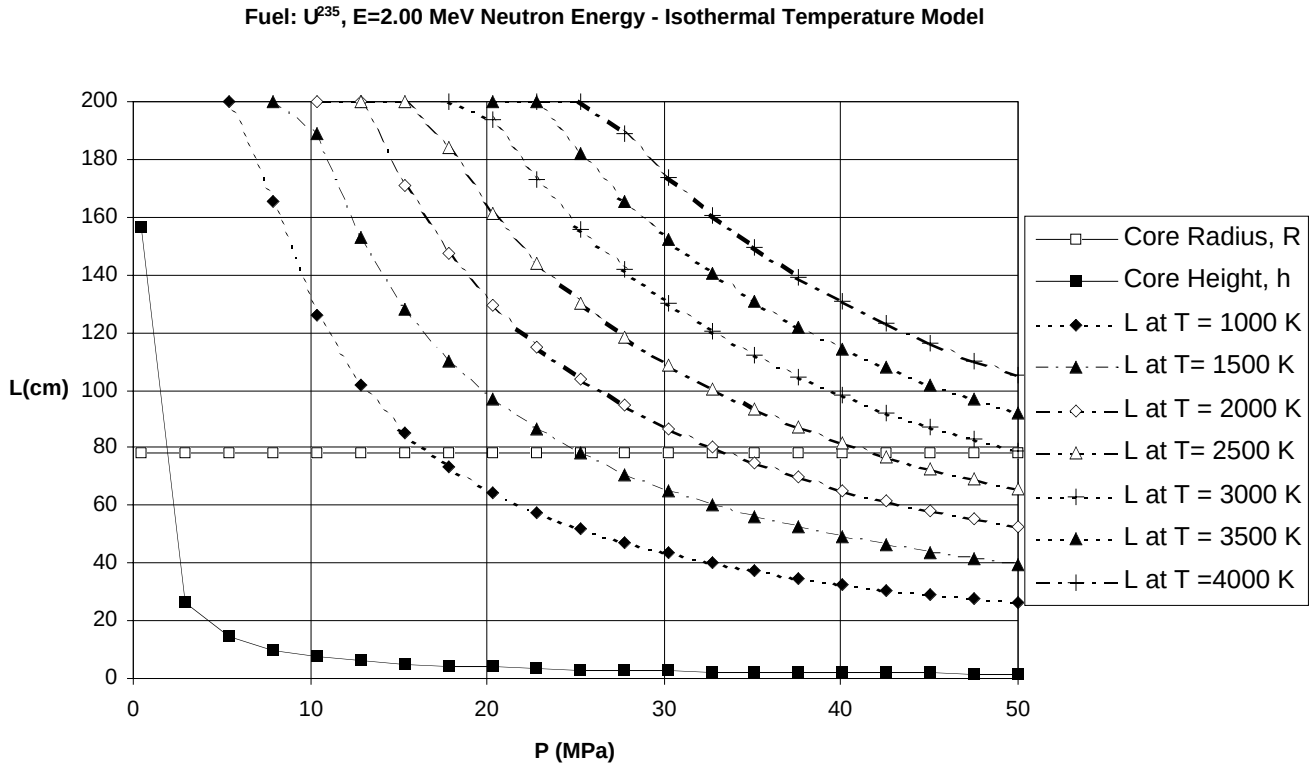

Figure 3-1. Diffusion Length, L, vs pressure, p, for U^{235} - Isothermal

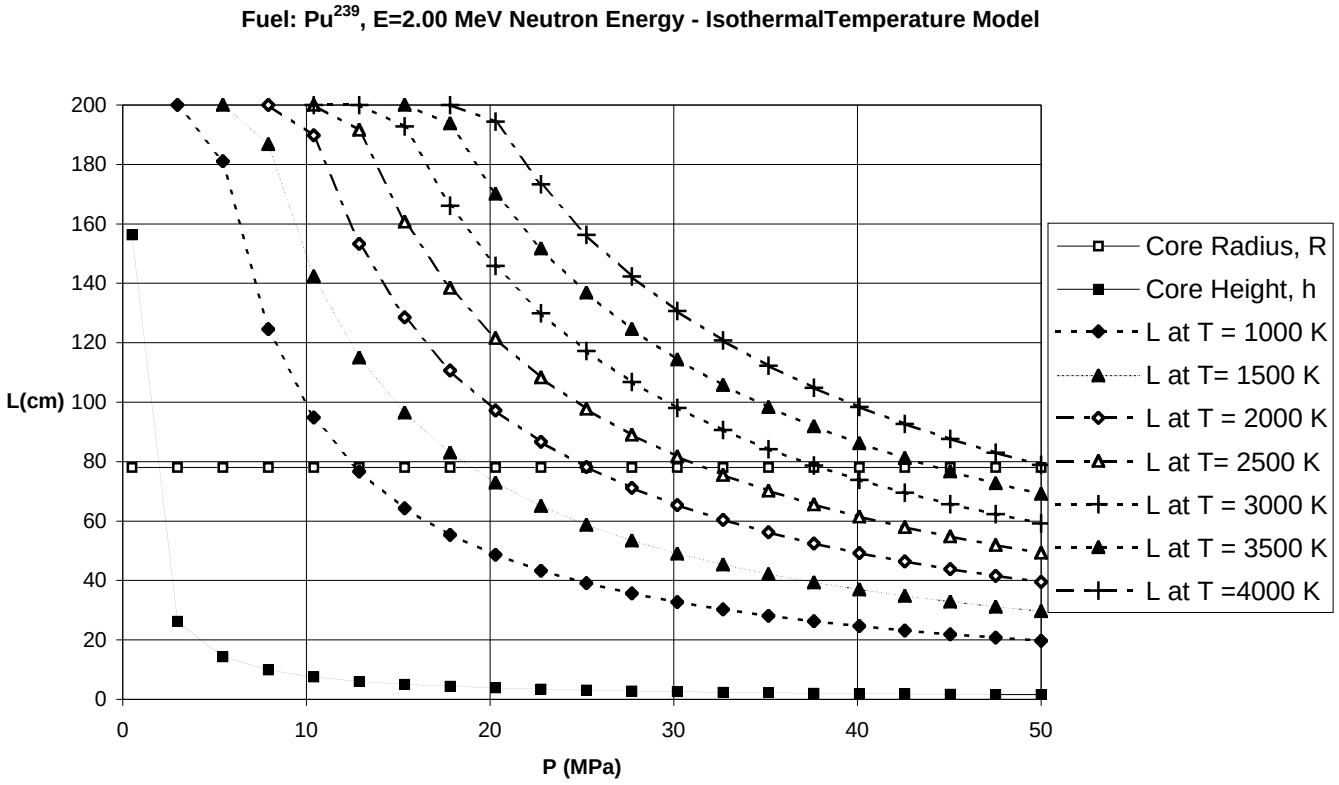

Figure 3-2. Diffusion Length, L, vs pressure, p, for Pu^{239} - Isothermal

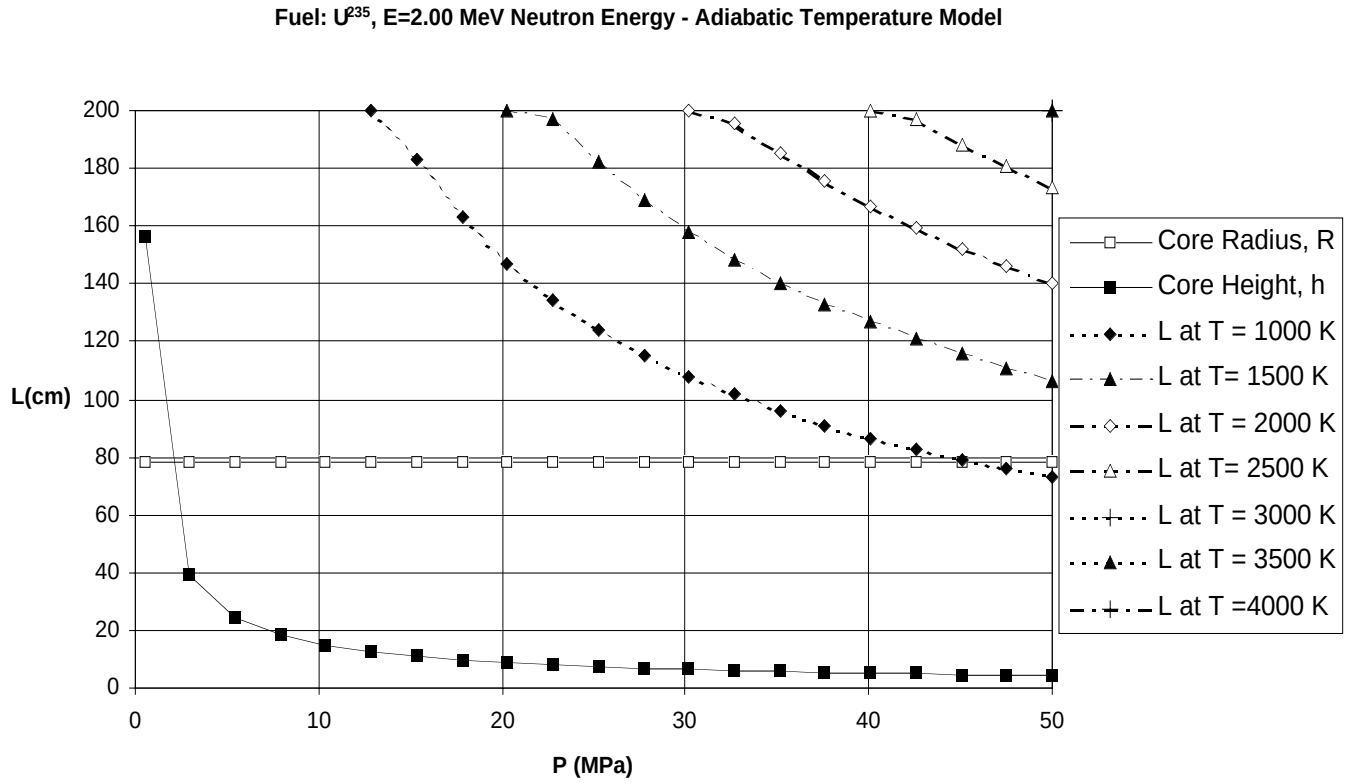

Figure 3-3. Diffusion Length, L, vs pressure, p, for U^{235} - Adiabatic

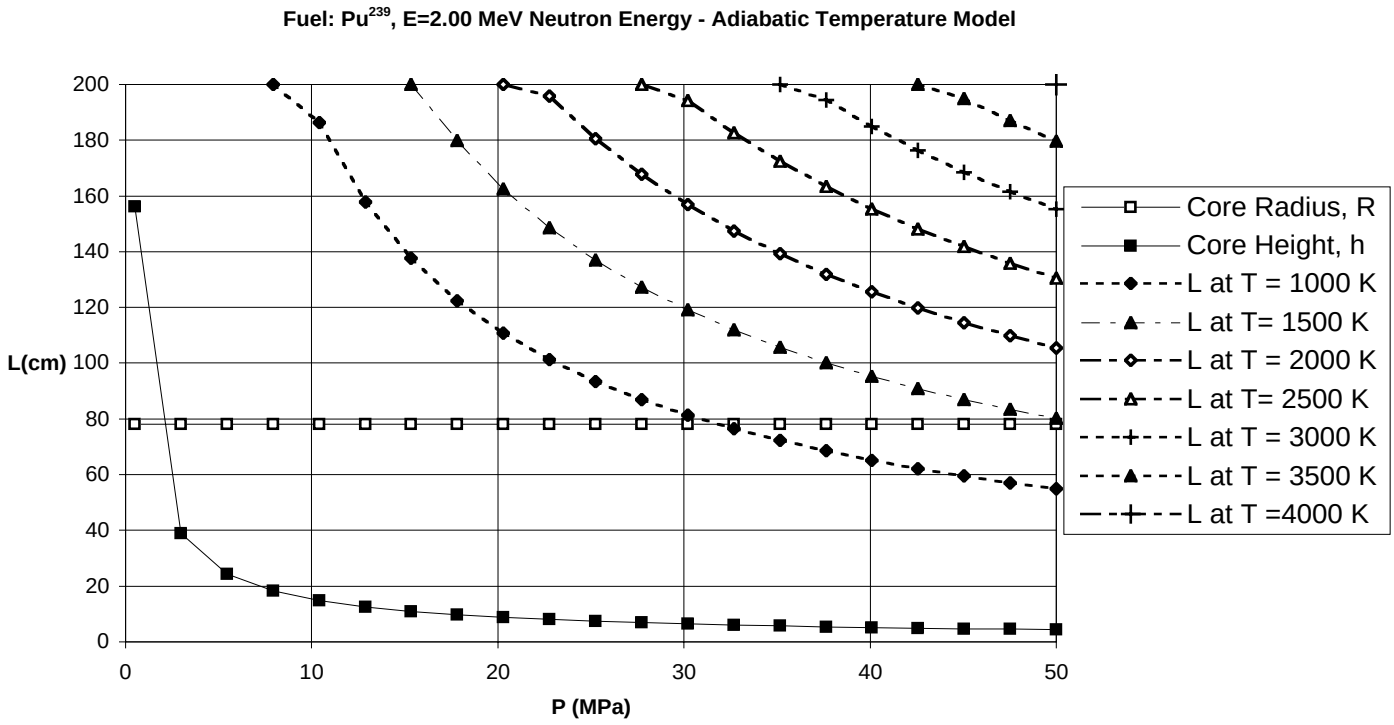

Figure 3-4. Diffusion Length, L, vs pressure, p, for Pu^{239} - Adiabatic

3.2 Core Material and Thermal Properties

To accurately calculate the core temperature that can be used to correct the reactivity, the thermal and materials properties must be accurately modeled. Improving the calculation of these material and thermal properties improves the calculation of the core temperature, T. The improved calculation of the core temperature can lead to an improved calculation of both the shroud temperature and the reflector temperature. These can lead to the detailed analysis and possible improvement of a number of design features of the FPCR.

These material and thermal properties include the molar specific heat, c_p, and the density, ρ, as well as the physical state of the core material. The molar specific heat is used to calculate the core heat capacity, (Mc_p), which is important in the calculation of the core temperatures. The core density is used to correct the reactivity and can be used in future thermal-hydraulic models as well. The state of the core material is important to determine the validity of calculation and for use in future thermal-hydraulic models.

3.2.1 Core Heat Capacity Calculation

The calculation of the core heat capacity, (Mc_p), is used in the calculation of the core temperature at the kth time step, T_{uk}, for each of the time steps. Furthermore, the core temperature at the kth time step, T_{uk}, may be used to provide a correction to the kinetics calculation at the kth time step and the initial temperature at the next time step. In order to calculate the core heat capacity, (Mc_p), the core volume, V_c, is calculated for a right circular cylinder:

$$V_c = \pi R^2 Z_c$$

Both the initial radius of the core, R, and the initial height of the core, Z_c, are user inputs.

Next, the number of moles of fuel in the core, N_{Mol}, is calculated for the time interval before the shock wave has begun compression. At this point, no nuclear heating has occurred. For simplicity, this is done using the Ideal Gas Law:

$$N_{Mol} = \frac{A_{MW}\, p_o V_c}{R_g T_0}$$

The constant, A_{MW}, is used to convert pressure from MPa to Pa and has the value of 1,000,000. The gas constant R_g has the value of 8.31441. The inlet temperature, T_0, is a user input.

The initial pressure, p_o, is a user input that is based on the results of MHD and MCNP simulations. Specifically, p_o is selected as the minimum value from the input pressure versus time table (developed from MHD calculations), or the effective multiplication factor versus pressure table (developed from MCNP calculations). The lowest pressure in these two tables is the value used as the initial pressure.

The core heat capacity, (Mc_p), is now calculated in the following manner:

$$(Mc_p) = N_{Mol} c_p R_g$$

The quantity, c_p, is the molar specific heat, which is a function of the core temperature for the kth time step, $T_{uk.}$ The calculation of the molar specific heat, c_p, is described in the next subsection.

3.2.2 Molar Specific Heat

The quantity, c_p, is the molar specific heat for the Actinide tetrafluoride, which is the specific heat for the Actinide tetrafluoride divided by the universal gas constant, R_0.

Originally, the molar specific heat for the Actinide tetrafluoride was approximated by half of the number of degrees of freedom of the molecule. This is equivalent to an ideal gas model:

$$c_p = 9/2$$

In the present, more empirical model, at relatively low core temperatures, T, which are below core temperatures where either ionization or disassociation occurs, the ideal gas model is again used. The Actinide (U, Pu, Th) tetraflouride molecules have nine degrees of freedom and therefore the molar specific heat, c_p, has the value

$$T \le T_{C0}$$
$$c_p = 9/2$$

where:

$$T_{C0} = 1000°K$$

For higher core temperatures, the empirical model[28] differs from the ideal gas model. For an intermediate range of core temperatures, T, the molar specific heat, c_p, is calculated in the following manner:

$$T_{C0} \le T \le T_{C2}$$
$$c_p = \frac{f_{cp0}}{R_0}(a_{cp01} + a_{cp11}T + \frac{a_{cp21}}{T^3})$$

The universal gas constant, R_0, used in this equation has the value

$$R_0 = 8.31441$$

The limiting temperature has the value

$$T_{C2} = 3500°K$$

The remaining quantities in this equation have the following values:

$$f_{cp0} = .31003352$$
$$a_{cp01} = 121.50$$
$$a_{cp11} = .00224$$
$$a_{cp21} = -3.06x10^9$$

[28] Thermophysical Properties of UF_4 at High Temperatures (1000 K ≤ T ≤ 10000 K) Samim Anghaie, University of Florida

For the upper range of core temperatures, T, the molar specific heat, c_p, is calculated in the following manner:

$$T_{C2} \leq T$$

$$c_p = \frac{f_{c0}}{R_0}(a_{cp02} + a_{cp12}T)$$

$$a_{cp02} = 124.12$$

$$a_{cp12} = .00128$$

The molar specific heat calculated using the empirical model is shown in Figure 3-5.

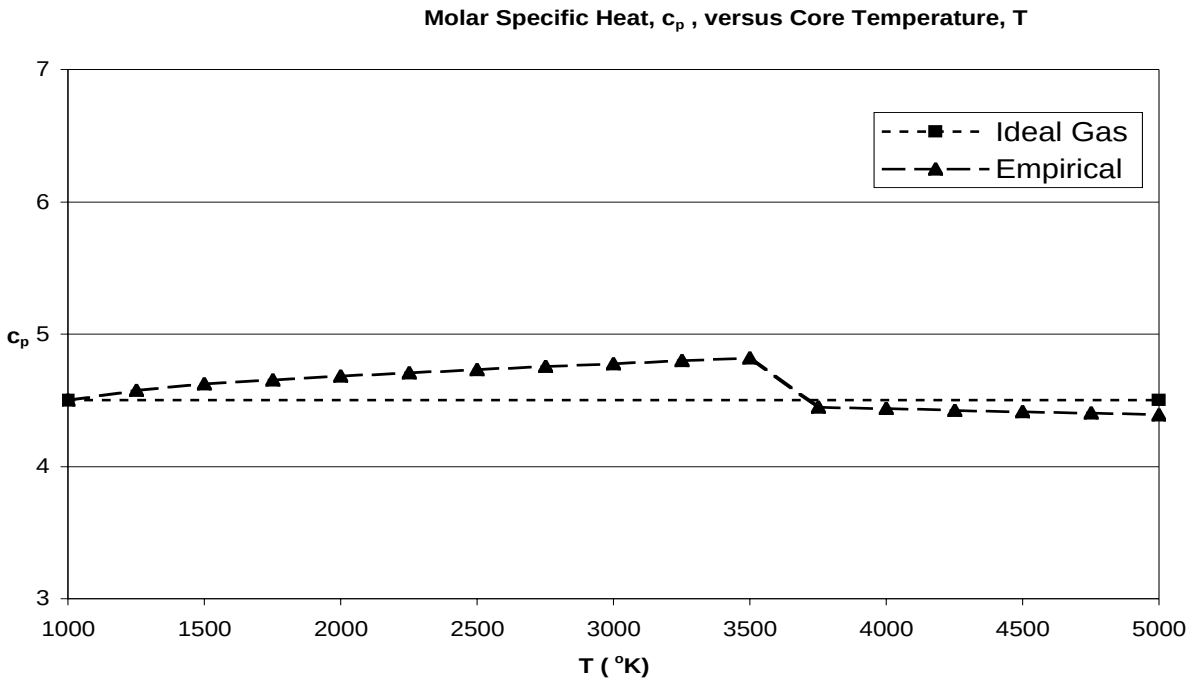

Figure 3-5. Molar Specific Heat, c_p, vs the core temperature, T

3.2.3 Density Calculation

The density of an Actinide (U, Pu, Th) tetraflouride gas is calculated as a function of the gas temperature, T, pressure, p, and the composition, using the universal gas law:

$$\rho_U = \frac{F_{Iso} A_{MW} p}{R_0 T}$$

The universal gas constant, R_0, is used in this equation and has the value

$$R_0 = 8.31441$$

The constant, A_{MW}, is used to convert the units of the density and has the value

$$A_{MW} = 1000000.00$$

The quantity, F_{Iso}, used to correct for the different isotopic weights of the three different isotopes, is simply the ratio of the mass of the isotope to the mass of U^{235}

Isotope	F_{Iso}
U^{233}	.99357
U^{235}	1.00000
Pu^{239}	1.01286

3.2.4 Testing the State of the Fluid in the Core

In the operation of the FPCR, it is assumed that the working fluid in the core is gaseous. However, due to the rapid increase in pressure, p, that assumption may be invalid. The testing the state of the fluid in the core is done by comparing the pressure, p, with the vapor pressure of UF4, $p_v(T)$, which is a function of the temperature, T. If the pressure exceeds the vapor pressure,

$$p > p_v(T)$$

the working fluid in the core is a liquid, not a gas, and a warning message is printed. If the pressure does not exceed the vapor pressure,

$$p \leq p_v(T)$$

the working fluid in the core is a gas, not a liquid.

For very high temperatures, where

$$T \geq T_{c5},$$

the vapor pressure is not calculated and the working fluid is assumed to be gaseous. For a lower range of temperatures, the vapor pressure, pv(T), will be the maximum of either the solid vapor pressure, $p_s(T)$, or the liquid vapor pressure, $p_l(T)$.

$$p_s(T) > p_l(T)$$
$$p_v(T) = p_s(T)$$

or

$$p_l(T) > p_s(T)$$
$$p_v(T) = p_l(T)$$

The solid vapor pressure, p_s, is calculated in the following manner for relatively low temperatures:

$$T \leq T_{v1}$$
$$a_p = a_{01} - \frac{R_{T01}}{T}$$
$$p_s(T) = \frac{C_{MPA} e^{a_p}}{T^{a_{11}}}$$

The quantity, C_{MPA}, has the value

$$C_{MPA} = 0.10135$$

The other constants in these equations are shown in Table 3-1. For higher temperatures, the solid vapor pressure, p_s, is calculated in the following manner:

$$T_{v1} \le T \le T_{v2}$$

$$a_p = a_{02} - \frac{R_{T02}}{T}$$

$$p_s(T) = \frac{C_{MPA} e^{a_p}}{T^{a_{12}}}$$

For even lower temperatures, the solid vapor pressure is assumed nonexistent:

$$T_{v1} < T$$

$$p_s(T) = 0$$

The liquid vapor pressure, p_l, is calculated in the following manner for relatively low temperatures:

$$T_{vi3} \le T \le T_{v4}$$

$$a_p = a_{0i} - \frac{R_{T03}}{T}$$

$$p_l(T) = \frac{C_{MPA} e^{a_p}}{T^{a_{31}}}$$

The liquid vapor pressure, p_l, is calculated in the following manner for higher temperatures:

$$T_{v4} \le T \le T_{v5}$$

$$a_p = a_{0i} - \frac{R_{T04}}{T}$$

$$p_s(T) = \frac{C_{MPA} e^{a_p}}{T^{a_{14}}}$$

Table 3-1 Constants Used in Testing the Fluid in the Core

i	Phase	$T_{vi}(^oK)$	a_{0i}	R_{T0i}	a_{1i}
1	Solid	900	20.300	16890.0	3.07
2		1309	47.659	39666.0	3.10
3	Liquid	1000	74.217	37977.0	7.00
4		1600	74.880	38453.0	7.05
5	Gas	3000	-	-	-

3.3 Core Temperature Models

Because of the dependence of the material properties on temperature, the calculation of the core thermal properties is a critical issue both in terms of safety and of the reliability of the FPCR. The calculation of the core thermal properties consists of three parts, the calculation of the two core temperature models and a comparison of the two core temperature models.

3.3.1 Adiabatic Temperature Model

The adiabatic temperature model is used to calculate the core temperature due to compression or expansion of the gas resulting from changes in pressure. It is only used if the user option, $I_{TMOD,}$ is set equal to 1.

$$I_{TMOD} = 1$$

The heat generated by nuclear reactions is not included in the adiabatic temperature model. In this model, the core temperature, T, is calculated from the pressure, p, and the initial core temperature, T_0, and the initial pressure, p_0.

The quantity, γ, is first calculated from the molar specific heat for the Actinide tetrafluoride, c_p, as described in a previous subsection, in the following manner:

$$\gamma = \frac{c_p}{c_p - 1}$$

Then the quantity, γ_0, is calculated:

$$\gamma_0 = \frac{\gamma - 1}{\gamma}$$

Then the initial ratio, τ_0, is calculated:

$$\tau_0 = \frac{T_0}{p_0^{\gamma_0}}$$

From these results, and the pressure, p, the core temperature, T, can be calculated:

$$T = \tau_0 p^{\gamma_0}$$

3.3.2 Isothermal Temperature Model

The isothermal temperature model, described in an earlier report[29], is included here for completeness and to facilitate a comparison between it and the adiabatic temperature model that has been introduced in this report. The isothermal temperature model is used only if the user option, $I_{TMOD,}$ is equal to 0.

$$I_{TMOD} = 0$$

The isothermal temperature model, used to calculate the core temperature, assumes that there is little or no change in the core temperature due to the compression or expansion of the gas resulting from changes in pressure. The heat generated by nuclear reactions is not included in the adiabatic temperature model. This model has been described previously but is included here for completeness and comparison with the adiabatic temperature model. In the isothermal temperature model, the core temperature, T, is calculated from the inlet temperature, T_0:

$$T = T_0$$

3.3.3 Comparison of the Temperature Models

A comparison between the adiabatic temperature model and the isothermal temperature model is shown in Figure 3-6. The pressure range used in this comparison is identical to the pressure range used in the FPCR reactor. The adiabatic temperature model predicts a much higher core temperature than is predicted by the isothermal temperature model.

A further comparison is provided by Figure 3-7 for U^{235} and Figure 3-8 for Pu^{239}. These two figures compare the core temperature rise due to the compression of the gas in the core of the FPCR. This comparison also shows that the adiabatic temperature model predicts a much higher core temperature than the isothermal temperature.

[29] FPCR Kinetics Feasibility Analysis In Progress Report, MAP-2002-V-F025-UNCLASS-050102, May 1, 2002

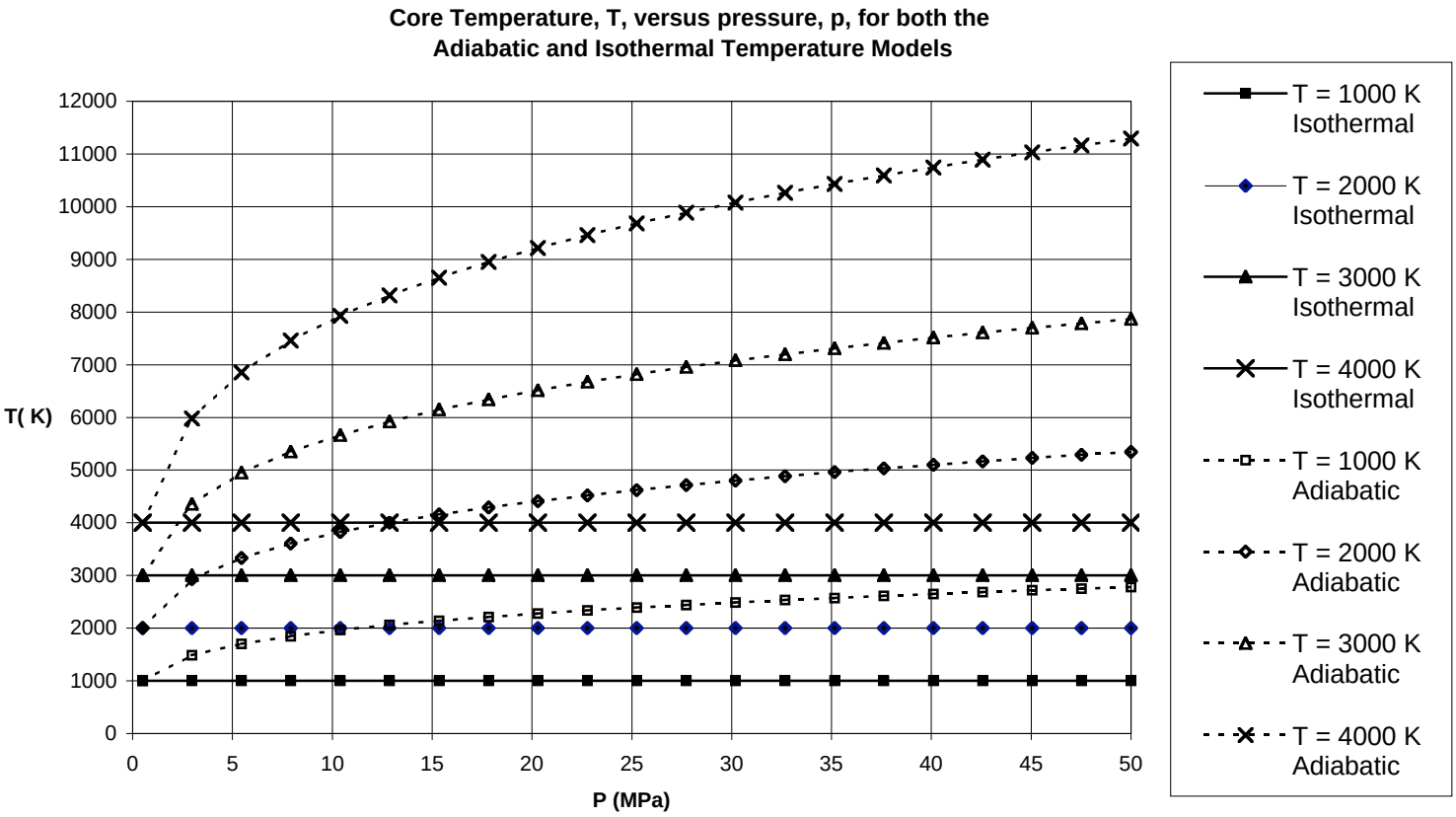

Figure 3-6. Comparison of the Two Temperature Models

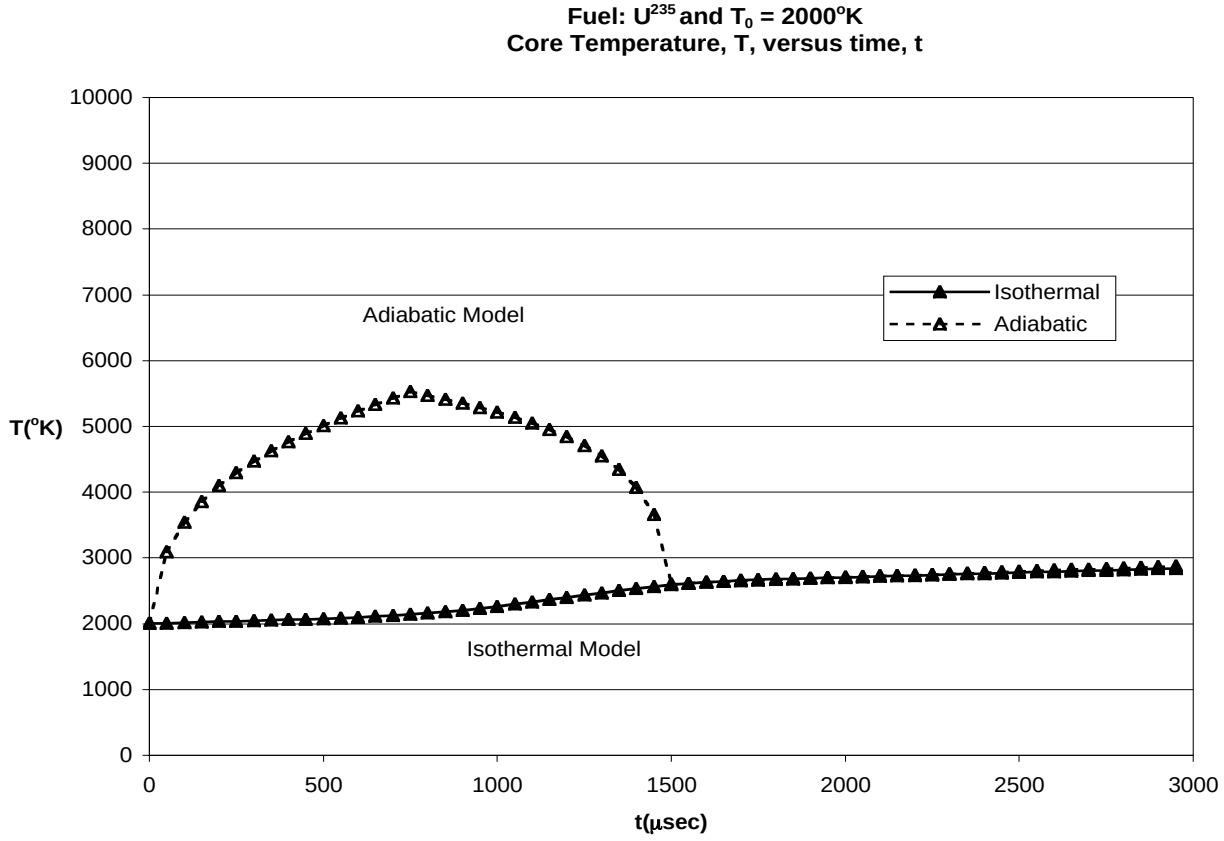

Figure 3-7. Transient Core Temperatures for both Temperature Models for U^{235}

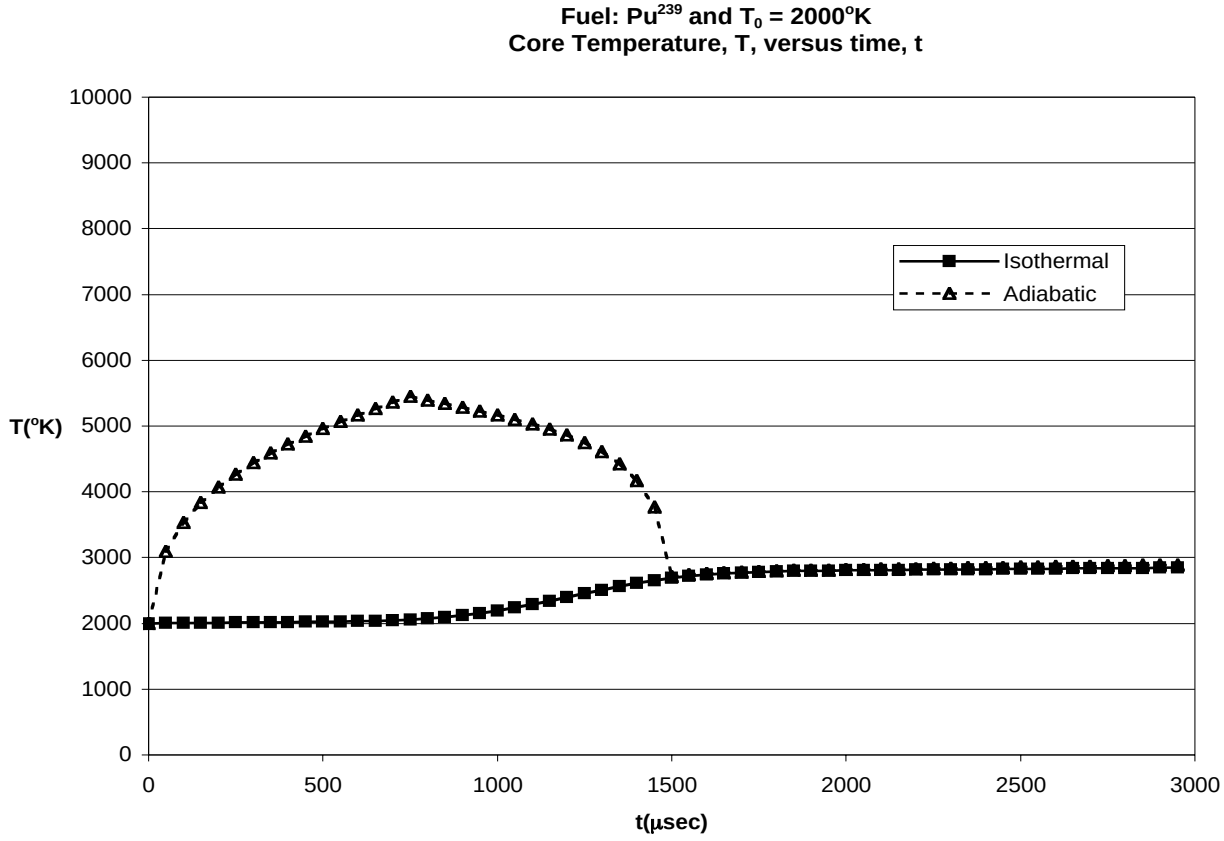

Figure 3-8. Transient Core Temperatures for both Temperature Models for Pu^{239}

3.4 Temperature/Density Reactivity Correction

The model used to correct the reactivity for changes in the density or temperature is determined by the option, I_{Cor}, which is part of the input requirements for the QCALC1 code and is explained in Appendix B. The calculation of the temperature/density reactivity correction is bypassed if the value of I_{Cor} is set equal to 0.

The first order temperature reactivity correction calculation is only performed if the option, I_{Cor}, is set equal to 1. These two possibilities are discussed previously.

Two additional models for the reactivity correction were added to the QCALC1 code. These two models are described in the next two subsections.

3.4.1 First Order Reactivity Density Correction

The first order density reactivity correction calculation is only performed if the option, I_{Cor}, is set equal to 2. The first order density reactivity is similar to the first order temperature reactivity, the major difference being that the gas density for the kth time step, ρ_{uk}, is used directly to calculate the corrected reactivity for the kth time step, ρ_{ck}, using linear interpolation:

$$\rho_{ck} = \rho_I(\rho_{uk})$$

The quantity, $\rho_I(\rho_{uk})$, represents linear interpolation with respect to the input density versus reactivity table. The calculation of the ith reactivity, ρ_{Ii}, which is used in this table was described previously. The ith density used in this table, ρ_{uIi}, is calculated initially using the ith pressure in the effective multiplication factor versus pressure table, p_{Ii}, and the inlet temperature, T_0:

$$\rho_{uIi} = \rho_U(T_0, p_{Ii})$$

The corrected reactivity for the kth time step, ρ_{ck}, is limited to the range

$$\rho_{Imin} \le \rho_{ck} \le \rho_{Imax}$$

The minimum reactivity, ρ_{Imin}, and maximum reactivity, ρ_{Imax}, are minimum and maximum values from the reactivity in the table.

Although the first order reactivity density correction is very accurate using the isothermal temperature model, it is extremely inaccurate if the adiabatic temperature model is used. Using the isothermal temperature model, the core temperature, T, is relatively close to the inlet temperature, T_0. This results in gas densities that are close to those in the input density versus reactivity table. Using the adiabatic temperature model, the temperature, T, can be much greater than the inlet temperature, T_0, resulting in gas densities that are much smaller than those in the input density versus reactivity table making interpolation for the reactivity difficult. For this reason, when the adiabatic temperature model is used, the first-order reactivity density correction is bypassed and the first-order reactivity temperature correction is used instead.

The effect of the first-order density reactivity correction on the corrected reactivity is shown in Figure 3-9 for U^{235} and Figure 3-10 for Pu^{239}. In these two figures, the corrected reactivity, calculated using the first order density reactivity correction, is significantly lower than the corrected reactivity with no correction despite the fact that both calculations use the isothermal temperature model. The effect of the first-order density reactivity correction on the power pulse is shown in Figure 3-11 for U^{235} and Figure 3-12 for Pu^{239}. Due to the lowered corrected reactivity, the first order density reactivity correction significantly lowers the peak power level.

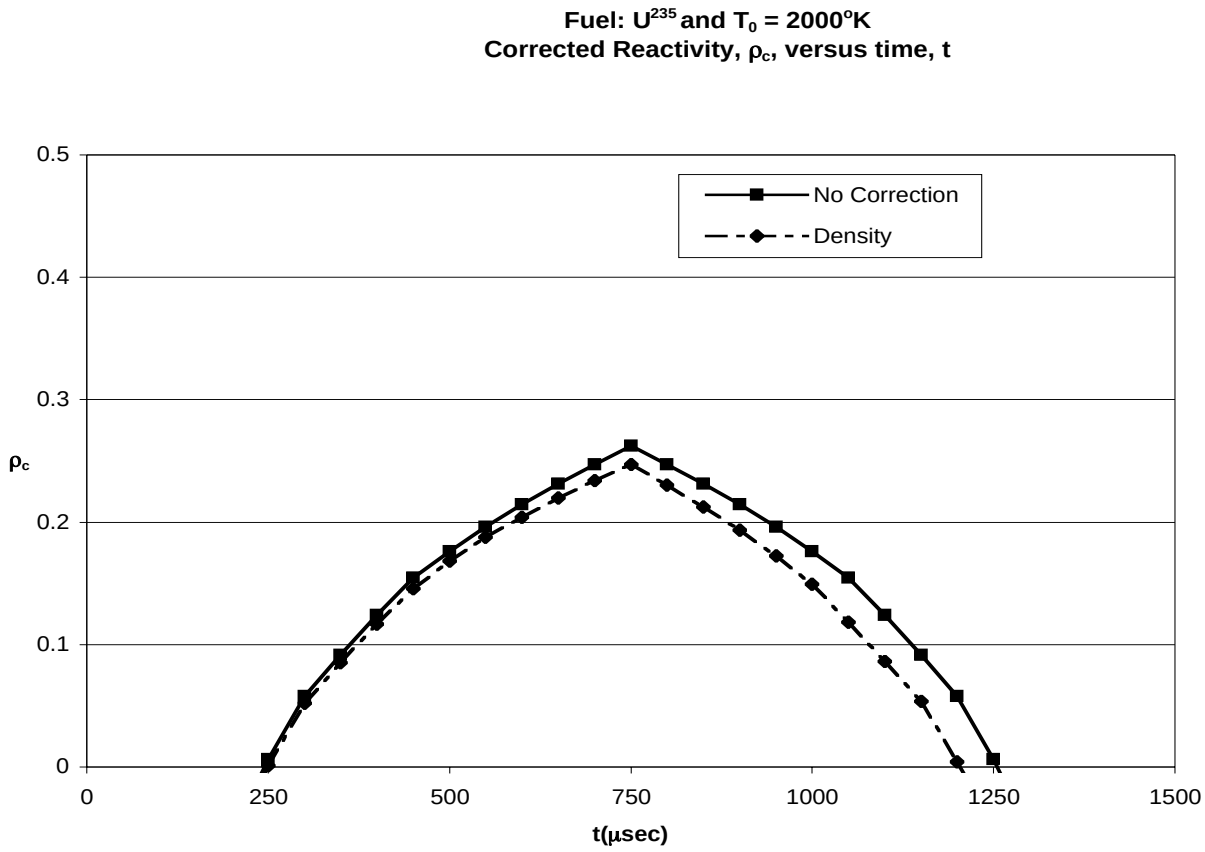

Figure 3-9. Effect of the Density Correction on the Corrected Reactivity for U^{235}

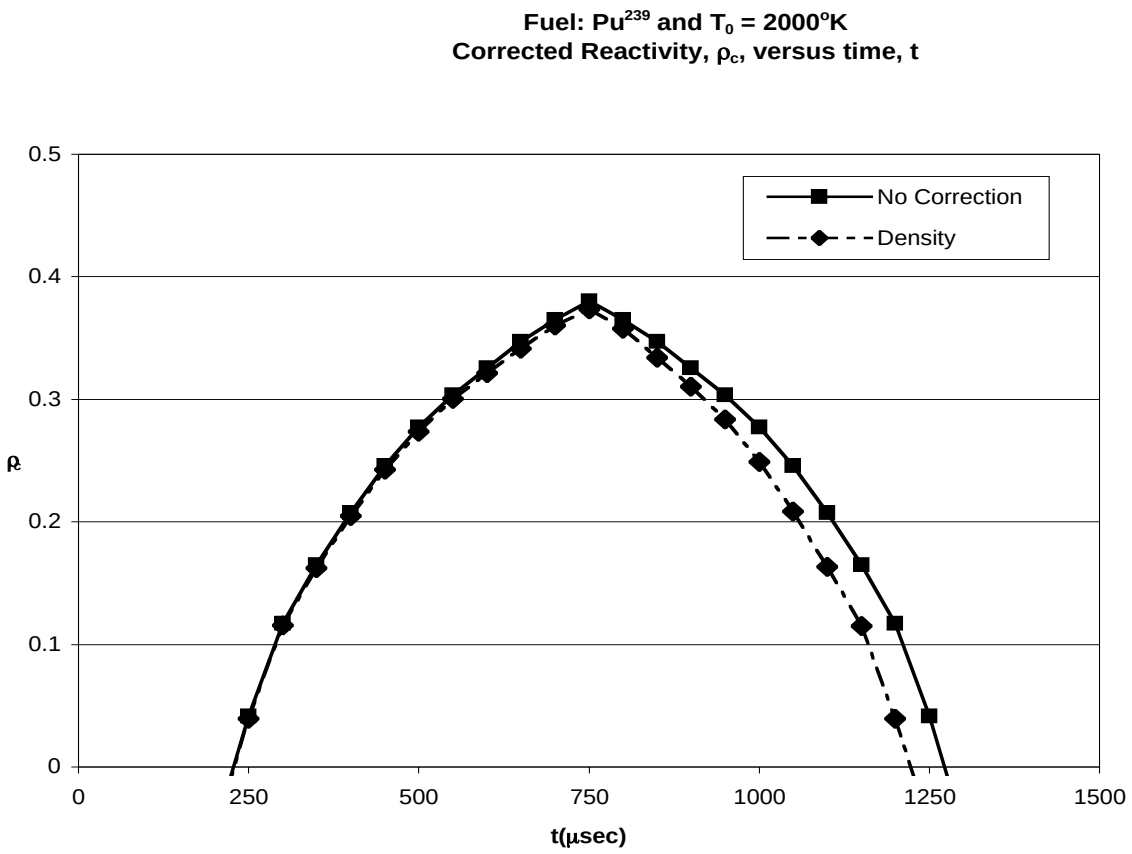

Figure 3-10. Effect of the Density Correction on the Corrected Reactivity for Pu^{239}

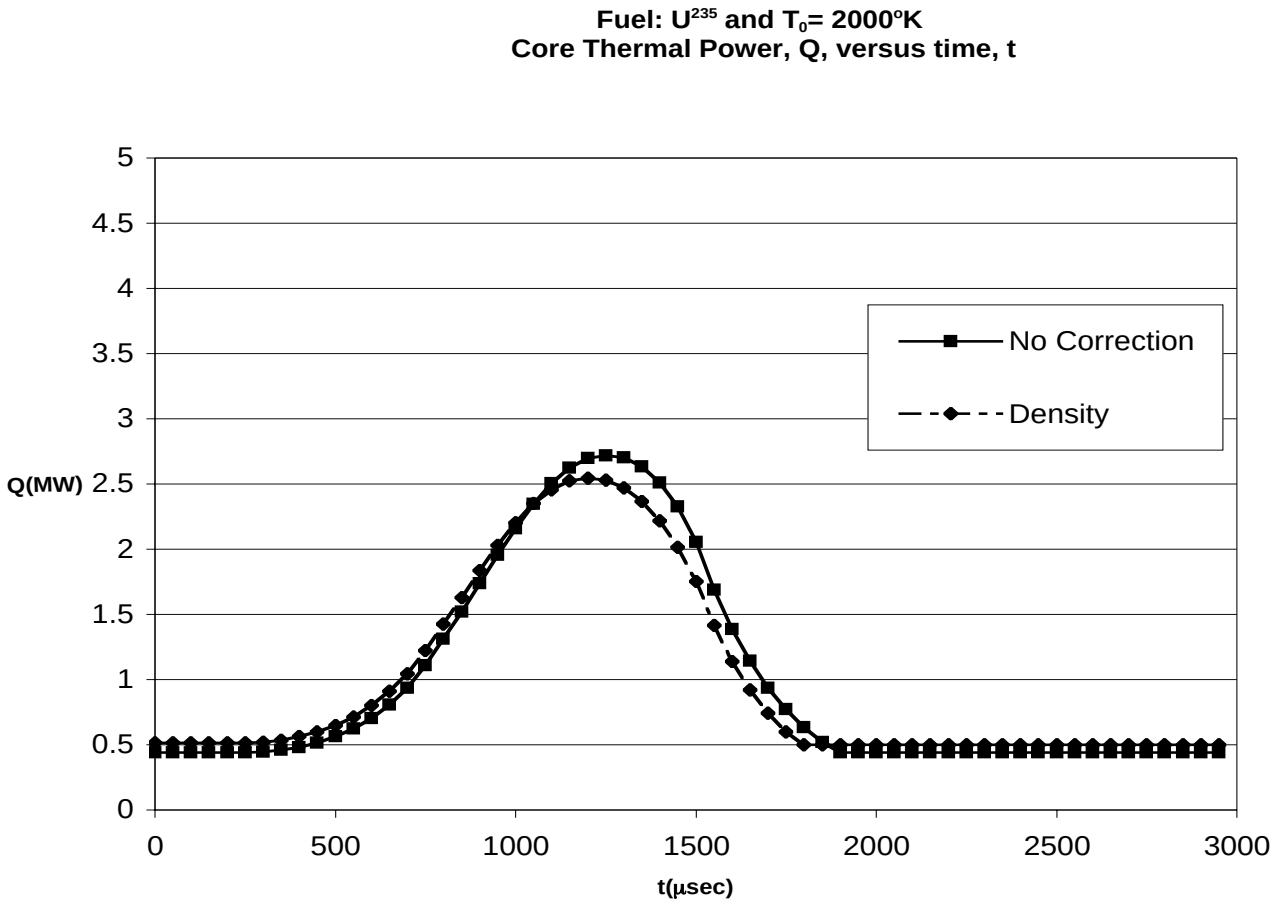

Figure 3-11. Effect of the Density Correction on the Power for U^{235}

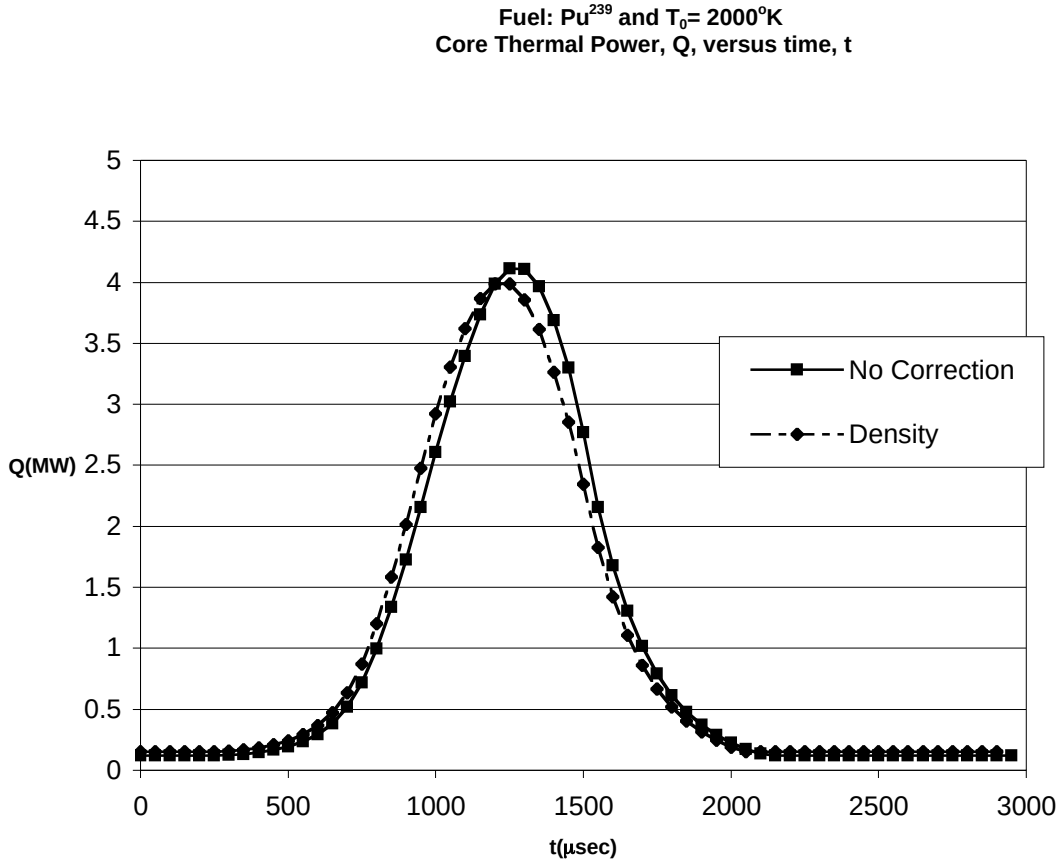

Figure 3-12. Effect of the Density Correction on the Power for Pu^{238}

3.4.2 Modifications to the First Order Reactivity Temperature Correction

The first order temperature reactivity correction calculation is only performed if the option, I_{Cor}, is set equal to one. The option, I_{Cor}, part of the input requirements for the QCALC1 code, is further explained in Section 4. If the first order temperature reactivity correction calculation is bypassed, the corrected reactivity at the kth time step, ρ_{ck}, is simply set equal to the reactivity at the kth time step, ρ_k:

$$I_{Cor} = 0$$

$$\rho_{ck} = \rho_k$$

If the first order temperature reactivity correction calculation is used, then the corrected reactivity at the kth time step, ρ_{ck}, is calculated in a manner that is similar to how the density is calculated in the MCNP4C code:

$$I_{Cor} = 1$$

$$\rho_{ck} = \rho(p_{effk})$$

The quantity, $\rho(p_{effk})$, is the reactivity obtained by linear interpolation from the reactivity versus pressure table. In these equations the effective pressure for the kth time step, p_{effk}, will be calculated differently, depending upon the temperature model used for the core fluid.

3.4.2.1 *Isothermal Temperature Model*

The isothermal temperature model, described in Subsection 3.3.2, is used only if the user option, I_{TMOD} is equal to 0; i. e.,

$$I_{TMOD} = 0$$

If the isothermal temperature model is used, then the effective pressure for the kth time step, p_{effk}, will be obtained from the pressure at the kth time step, p_k, and the inlet temperature, T_0, and the core temperature at the kth time step, T_{uk}, in the following manner:

$$p_{effk} = \frac{T_0 p_k}{T_{uk}}$$

3.4.2.2 *Adiabatic Temperature Model*

The adiabatic temperature model is described in Subsection 3.3.1 and used only if the user option, I_{TMOD} is equal to 1; i. e.,

$$I_{TMOD} = 1$$

Because the dependence of the gas density on the pressure is different for the adiabatic temperature model, a significantly different method is used to calculate the effective pressure, p_{eff}, in the reactivity temperature correction. Firstly, the average molar specific heat, c_{pav}, is calculated by averaging the molar specific heats at the inlet, $c_p(T_0)$, and at the present time step, $c_p(T_u)$, in the following manner:

$$c_{pav} = \frac{1}{2}[c_p(T_0) + c_p(T_u)]$$

The quantity, γ, is calculated from the average molar specific heat for the Actinide tetrafluoride, c_{pav}, using the following:

$$\gamma = \frac{c_{pav}}{c_{pav} - 1}$$

Then, the quantity, α,is calculated in the following manner:

$$\alpha = \gamma - 1$$

The effective pressure, p_{eff}, in the reactivity temperature correction can now be calculated from the pressure for the kth time step, p_k:

$$p_{eff} = \left(\frac{T_0}{T_u}\right)^{\alpha} p_k$$

$$\gamma_0 = \frac{\gamma - 1}{\gamma}$$

3.4.2.3 *Effect of the Temperature Models on the Power*

The effect of the isothermal and the adiabatic temperature models on the corrected reactivity is shown in Figure 3-13 for U^{235} and in Figure 3-14 for Pu^{239}. In both of these figures, the corrected reactivity calculated using the adiabatic temperature model is very significantly lower compared to the corrected reactivity calculated using the isothermal temperature model. The much higher core temperature calculated by the adiabatic temperature model lowers the corrected reactivity compared to the corrected reactivity calculated using the isothermal temperature model. A comparison between the temperatures predicted by the adiabatic temperature model and those predicted by the isothermal model is in Figure 3-7 for U^{235} and Figure 3-8 for Pu^{239}.

The effect of both of the temperature models on the power is shown in Figure 3-15 for U^{235} and in Figure 3-16 for Pu^{239}. The power predicted using the adiabatic temperature model is significantly lower than the power predicted by the isothermal temperature model. This is due to the lowered value of the reactivity calculated by the adiabatic temperature model, compared to the reactivity calculated using the isothermal temperature model.

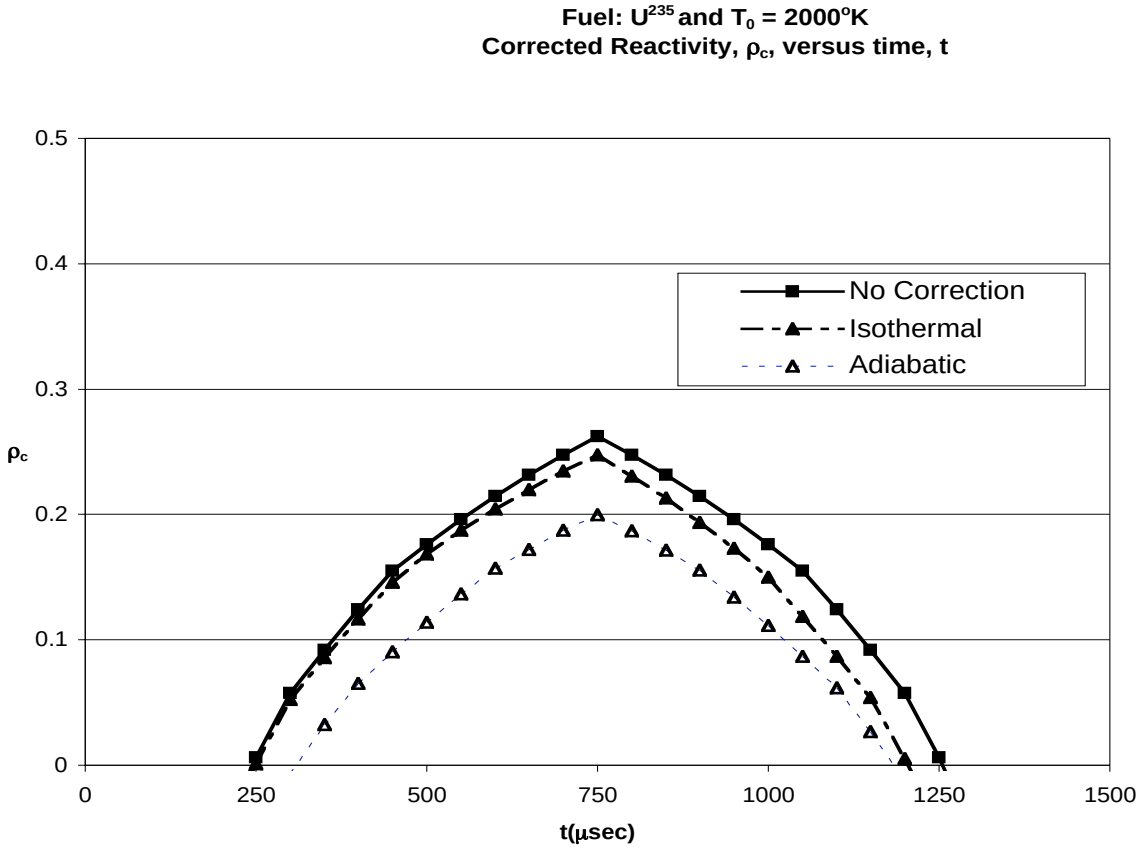

Figure 3-13. Effect of the Temperature Model on the Corrected Reactivity for U^{235}

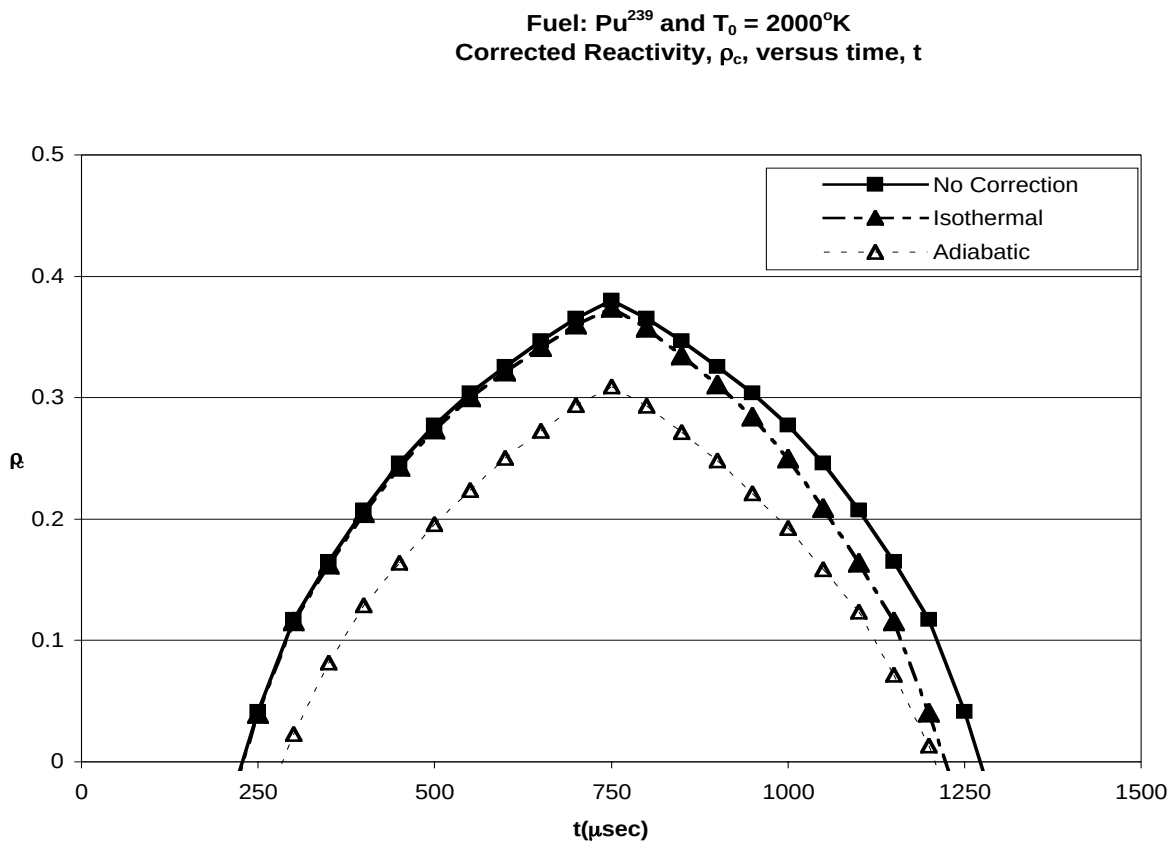

Figure 3-14. Effect of the Temperature Model on the Corrected Reactivity for Pu^{239}

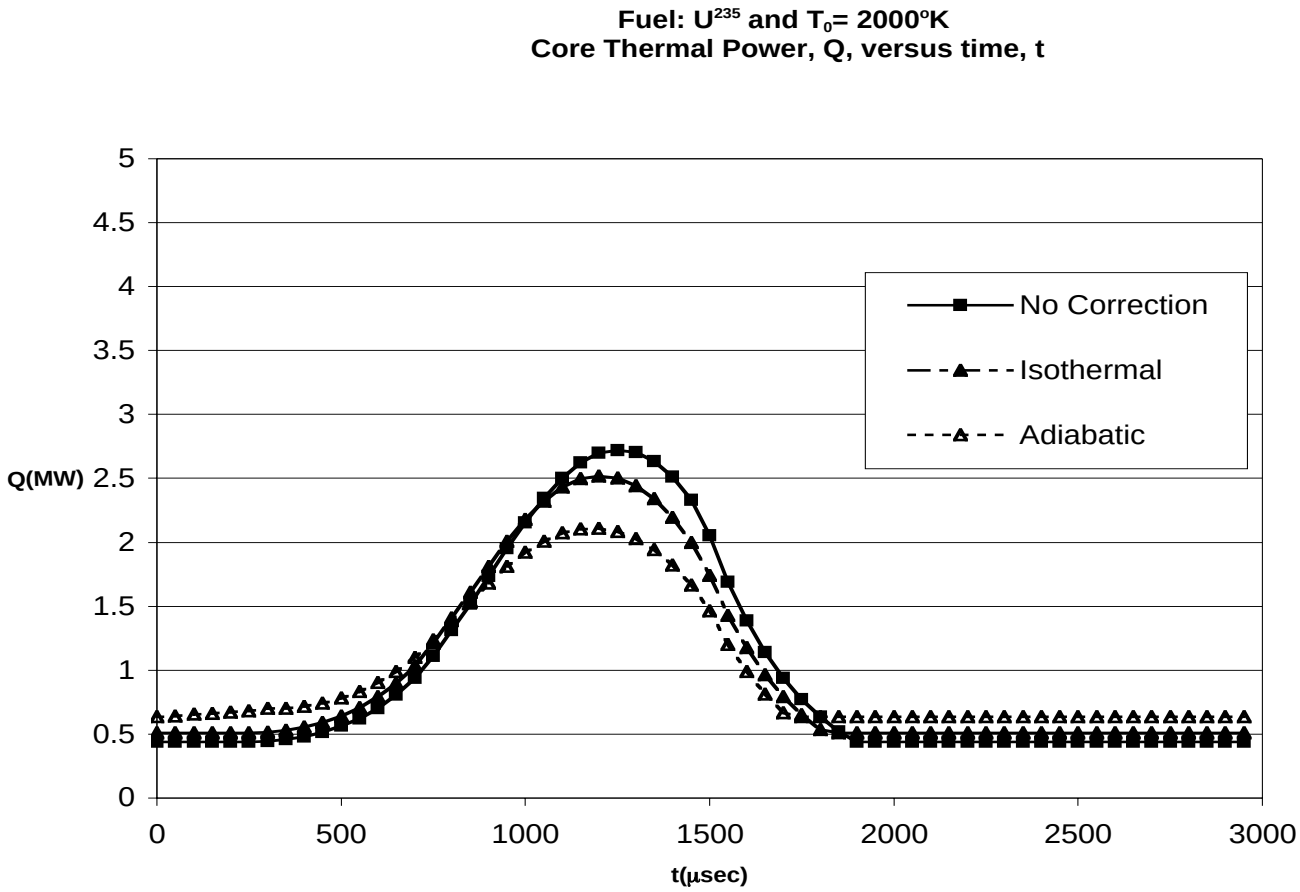

Figure 3-15. Effect of the Temperature Models on the Power for U^{235}

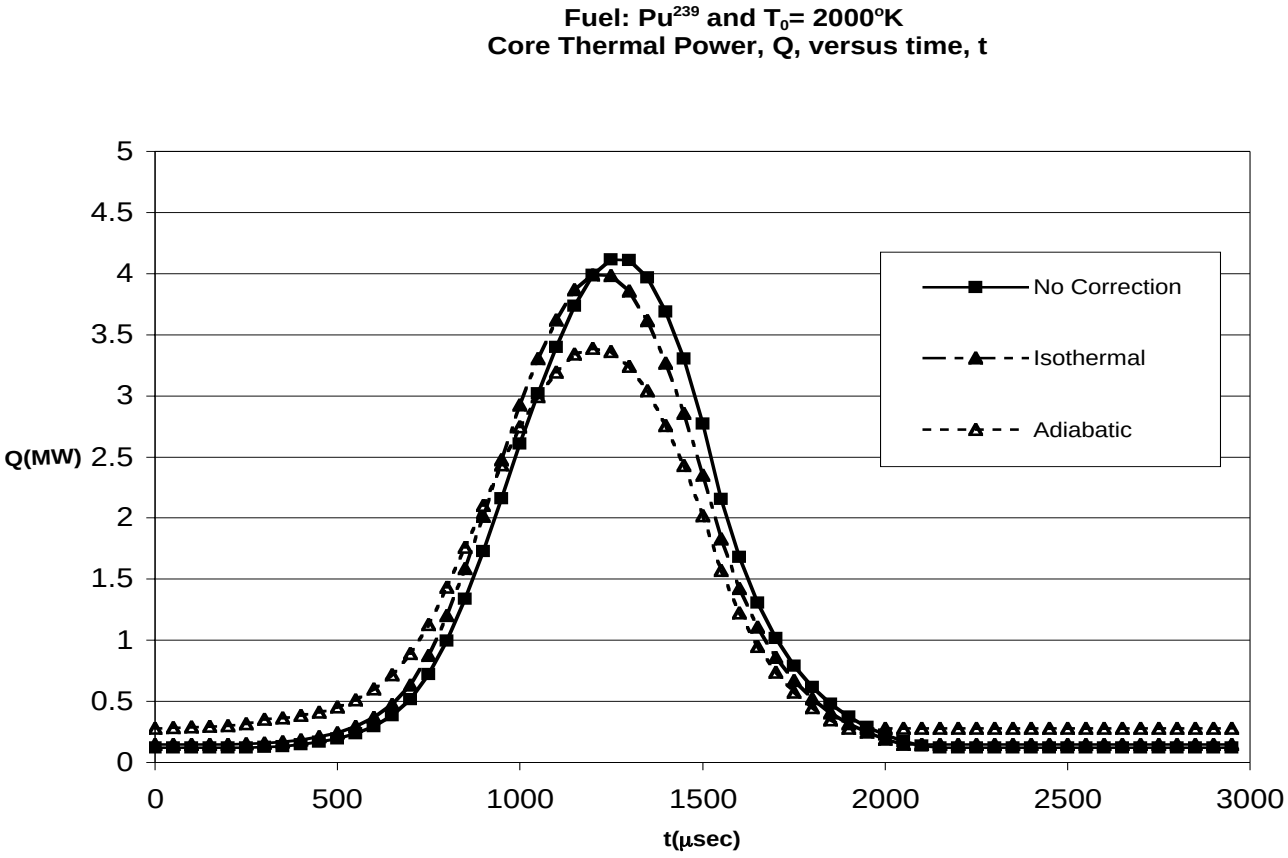

Figure 3-16. Effect of the Temperature Models on the Power for Pu^{239}

3.5 Further Improvements to the QCALC1 Code

Although the capabilities of the QCALC1 code are numerous, additional models should be added to the code to increase its capabilities. This would enable the QCALC1 code to perform additional types of analyses that are directly related to the dynamic, pulsing nature of the FPCR. These modifications include a calculation of an increased number of pulse shape parameters, the calculation of the shroud temperature and its effect on the integrity of the shroud and a modification of the input requirements to be compatible with other core physics codes.

The pulse shape parameters are important because the information provided about the power pulse is relatively concise and easily understood. Two pulse shape parameters, the maximum power and the corrected maximum power, are already calculated by the QCALC1 code; these have been found to be very useful in the comparison of various core designs. The additional calculation of a bandwidth parameter and a signal to noise ratio parameter would also facilitate the comparison of core designs and provide useful information in a form more compatible with the needs of the design of the MHD system.

A model for both the average temperature of the shroud and the maximum temperature of the shroud can be implemented. Models for the melting point, the yield stress, and the hoop stress can also be implemented. Using all of these models, the mechanical and thermal integrity of the shroud can be estimated accurately.

The outputs of the two supplemental core physics codes, VENTURE and KENO, may differ somewhat from that of MCNP4C. If this difference is significant then another set of input requirements may be required for the each of the supplemental codes. This is necessary to ensure the accuracy of the kinetics calculations and increase the speed of the preparation of input data by minimizing the number of hand calculations for input data preparation.

4 SUMMARY AND CONCLUSION

Detailed and accurate core physics calculations have been performed using the MCNP4C code system. These calculations have demonstrated both the feasibility of the core design for the FPCR and have determined the feasibility of at least two fissile isotopes, U^{235} and Pu^{239}, for possible use as fuels. Since the use of a number of core physics code systems is necessary, the COMBINE/VENTURE code system, and the SCALE4a.a code system, should be used in conjunction with the MCNP4C code to increase the accuracy and the flexibility of the calculation. Efforts to build accurate FPCR models for these code systems have begun; some preliminary calculations were performed with the COMBINE code. Input data sets for both the VENTURE code and the SCALE4a.a code system were started, including the development of an input data generation code, SIZE1, to provide temperature and pressure dependent input data for both of these code systems.

The kinetics code, QCALC1, has been substantially improved. These improvements include improved material properties to the model, the implementation of a more accurate adiabatic core temperature model. The first order reactivity correction has been modified to properly interface with these improvements. All of these improvements to the QCALC1 have been extensively tested. Although further improvements to the QCALC1 code are desired, the improvements described here have increased the accuracy of the kinetics methodology and calculations.

The nuclear engineering staff at the Institute for Scientific Research has developed an accurate core and kinetics modeling system that will be useful in further feasibility and design studies for the FPCR.

APPENDIX A QCALC1 SUBROUTINE DESCRIPTION

The QCALC1 code consists of a number of subroutines. This section provides a description of each of these subroutines.

QCALC1: Main program. Reads input data and writes out results. Calculates the duration of the calculation and selects the time points. Calculates the reactivity at each pressure point and at each time point, the heat per cycle, the normalized power, the core thermal power, the core temperature, and the pulse shape parameters. Writes the output files including printed output, summary output file, EXCEL plot file, and the LINUX plot files. Calls PCALC, RHOCALC, RHOCORR0, RHOCORR1, QSUBEQU, RHOUF4, ADIABAT, GASTEST, QSPECIFIC, MINMAX, POINT1, PROMPT1, KINMAX, KINMIN.

PCALC: Calculates the time points on the pressure versus effective multiplication factor input data curve from the pressure versus time table.

RHOCALC: Calculates the reactivity and pressure at each time step.

RHOCORR0: Calculates the first order temperature corrected reactivity for each time step.

RHOCORR1: Calculates the first order density corrected reactivity for each time step.

NEWTON: Uses Newton's method to solve the reactivity equation for the inverse period at each time step.

POINT1: Selects the models used in the calculation of the normalized power with the point kinetics model. Calls QRAMP, NEWTON, SCRAM1 and QSUBEQU.

PROMPT1: Selects the models used in the calculation of the normalized power with the prompt jump model. Calls QRAMP, JUMP1, SCRAM1 and QSUBEQU.

KINMAX: Selects the models used in the calculation of the maximum normalized core power curve with either the prompt jump model or the point kinetics model. Calls QRAMP, NEWTON, JUMP1, SCRAM1 and QSUBEQU.

KINMIN: Selects the models used in the calculation of the minimum normalized core power curve with either the prompt jump model or the point kinetics model. Calls QRAMP, NEWTON, JUMP1, SCRAM1 and QSUBSEQU.

JUMP1: Calculates the normalized power from the reactivity using the prompt jump method.

QRAMP: Calculates the normalized power using the dynamic subcritical model at each time point from the delayed neutron fractions and the reactivity at each time step.

QSUBEQU: Calculates the normalized power using the equilibrium subcritical model each time point from the delayed neutron fractions and the reactivity at each time step.

SCRAM1: Calculates the normalized power at each time step immediately after super criticality for rapidly changing negative reactivity.

XYLOC: Positions the parts of the legend in the LINUX plots.

CULL1: Eliminates superfluous data points in the LINUX plots.

ADIABAT: Calculates the transient core temperature using the adiabatic model. Calls QSPECIFIC.

QSPECIFIC: Calculates the molar specific heat of gaseous UF_4.

GASTEST: Tests to determine whether the core fluid is gaseous or liquid.

RHOUF4: Calculates the density of the core fluid as a function of the temperature, pressure and isotope mass.

MINMAX: Obtains the minimum and maximum pressures and densities.

APPENDIX B QCALC1 USER INFORMATION

This section is intended to provide sufficient information to enable calculations with the QCALC1 code. Included are the input requirements of QCALC1 and the execution procedure.

B.1 INPUT REQUIREMENTS

All of the input requirements for the QCALC1 code are presented in Table B-1 through Table B-5. The *Card #* column locates the input data in the QCALC1 input data set. The *Input Variable* column tells the name of the variable in the QCALC1 code. The *Symbol* column describes the symbol used for the input data in the equations in the theory section of Reference 1 and this section. The *Format* column gives the format of the input data. The *Description* column describes the required input data and the *Units* column describes the units of the required input data.

The listings of the input data sets in Appendix B.4 provide an example for entering input data.

Table B-1. Input Requirements – Titles and Options

Card No.	Input Variable	Symbol	Format	Description	Units
1	**TITLE1**	-	A80	Case Title	-
2	**SUFFIX7**	-	A4	Last 4 characters of the name of the file containing the input data for plotting using EXCEL, make this different for every case run	-
3	**NP**	N_p	I10	Number of points in the pressure versus time table	-
	NK	N_k	I10	Number of points in the effective multiplication factor versus pressure table	-
	M	M	I10	Input isotope index for the delayed neutron data m=0 read in delayed neutron data m=1 use U^{233} thermal neutron spectrum m=3 use Pu^{239} thermal neutron spectrum m=4 use U^{233} prompt neutron spectrum m=5 use U^{235} prompt neutron spectrum m=6 use Pu^{239} prompt neutron spectrum	-
	ICOR	I_{cor}	I10	Indicator for use of the first order temperature reactivity correction I_{cor}=0 No first order reactivity correction used I_{cor}=1 The first order temperature reactivity correction used I_{cor}=2 The first order density reactivity correction used	-
	IKIN	I_{kin}	I10	Indicator for the model set used I_{kin}=1 Point kinetics model set used I_{kin}=2 Prompt jump model set used I_{kin}=3 Maximum power model set used I_{kin}=4 Minimum power model set used	-
	ITMOD	I_{TMOD}	I10	Indicator for the temperature model used I_{TMOD}=0 Isothermal temperature model used I_{TMOD}=1 Adiabatic temperature model used	

Table B-2. Input Requirements – Output and Plotting Options

Card No.	Input Variable	Symbol	Format	Description	Units
4	**IPRNT**	I_{prnt}	I10	Indicator for the amount of printed output I_{prnt}=0 Summary output only I_{prnt}=1 Detailed and Summary output I_{prnt}=2 Detailed and Summary output at all time steps	-
	IPLOT	I_{plot}	I10	Indicates the plotting options used I_{plot}=0 none I_{plot}=1 LINUX full plots only I_{plot}=2 LINUX full plots and EXCEL plot files I_{plot}=3 LINUX partial plots only to the first set of partial plot files I_{plot}=4 LINUX partial plots only to the second set of partial plot files I_{plot}=5 LINUX partial plots only to the third set of partial plot files I_{plot}=6 EXCEL plot files only I_{plot}=7 LINUX partial plots to the first set of partial plot files and EXCEL plot files I_{plot}=8 LINUX partial plots to the second set of partial plot files and EXCEL plot files I_{plot}=9 LINUX partial plots to the third set of partial plot files and EXCEL plot files	-
	ILINE	I_{line}	I10	Indicates the type of line used I_{line}=0 none I_{line}=1 solid line, _____ I_{line}=2 dashed line, _ _ _ _ _ I_{line}=3 dotted line, ...	-
	IDATA	I_{data}	I10	I_{data}=0 none I_{data}=1 circle, o I_{data}=2 box, I_{data}=3 ellipse, ◊ I_{data}=4 plus, +	-
	ILOC	I_{loc}	I10	Indicates line location in the legend I_{data}=1 is at the top of the legend	-

Table B-3. Input Requirements – LINUX Plot Scaling Options

Card No.	Input Variable	Symbol	Format	Description	Units
				(Card 5 is used only if $1 \le I_{plot} \le 5$ or $7 \le I_{plot} \le 9$)	
5	**IDUR**	I_t	I10	Transient plot duration indicator I_t=0 no set duration I_t=1 1000 sec duration I_t=2 2000 sec duration I_t=3 3000 sec duration I_t=4 5000 sec duration I_t=5 10000 sec duration	-
	IQMAX	I_{Qmax}	I10	Maximum power range indicator I_{Qmax}=0 no set minimum scale I_{Qmax}=1 2.25 kw minimum scale I_{Qmax}=2 4.50 kw minimum scale I_{Qmax}=3 9.00 kw minimum scale I_{Qmax}=4 18.00 kw minimum scale I_{Qmax}=5 36.00 kw minimum scale	-
	ITMAX	I_{Tmax}	I10	Temperature range indicator I_{Tmax}=0 no set minimum scale I_{Tmax}=1 500 K $\le T_u \le$1400 K I_{Tmax}=2 500 K $\le T_u \le$ 2750 K I_{Tmax}=3 1000 K $\le T_u \le$ 5500 K I_{Tmax}=4 1000 K $\le T_u \le$ 10000 K I_{Tmax}=5 2000 K $\le T_u \le$ 20000 K	-
	IRMAX	I_{max}	I10	I_{max}=0 no set minimum scale I_{max}=1 -0.100 $\le \rho_c \le$ 0.125 I_{max}=2 -0.200 $\le \rho_c \le$ 0.250 I_{max}=3 -0.400 $\le \rho_c \le$ 0.500 I_{max}=4 -0.800 $\le \rho_c \le$ 1.000	-

Table B-3. Input Requirements – Plotting Information (Continued)

Card No.	Input Variable	Symbol	Format	Description	Units
				(Card 5 is used only if $1 \le I_{plot} \le 5$ or $7 \le I_{plot} \le 9$)	
5 (cont)	**IPMAX**	I_{pmax}	I10	Pressure range indicator $I_{pmax} = 0$ no set minimum scale $I_{pmax} = 1$ $0 \le p \le 18$ MPa $I_{pmax} = 2$ $0 \le p \le 45$ MPa $I_{pmax} = 3$ $0 \le p \le 90$ MPa	-
	IKMAX	I_{kmax}	I10	Effective multiplication factor range indicator $I_{kmax} = 0$ no set minimum scale $I_{kmax} = 1$ $k_{eff} \le 1.500$ $I_{kmax} = 2$ $k_{eff} \le 2.000$ $I_{kmax} = 3$ $k_{eff} \le 2.500$	-
	ILMAX	I_{Lmax}	I10	$I_{Lmax} = 0$ no set minimum scale $I_{Lmax} = 1$ $L_p \le 0.360$ msec $I_{Lmax} = 2$ $L_p \le 0.720$ msec $I_{Lmax} = 3$ $L_p \le 1.440$ msec	-

Table B-4. Input Requirements – Figure Numbering Information

Card No.	Input Variable	Symbol	Format	Description	Units
				(Card 6 is used only if $1 \le I_{plot} \le 5$ or $7 \le I_{plot} \le 9$)	
6	**DTOFF**	Δt_{off}		Time offset used to align important features for multiple sets of results	-
	FIG1	N_{Fig1}	F10.5	Figure number for the power versus time plot $N_{Fig1} \le 0$ Suppress the figure number $N_{Fig1} > 0$ Include the figure number	-
	FIG2	N_{Fig2}	F10.4	Figure number for the temperature versus time plot $N_{Fig2} \le 0$ Suppress the figure number $N_{Fig2} > 0$ Include the figure number	
	FIG3	N_{Fig3}	F10.4	Figure number for the reactivity versus time plot $N_{Fig3} \le 0$ Suppress the figure number $N_{Fig3} > 0$ Include the figure number	
	FIG4	N_{Fig4}	F10.4	Figure number for the pressure versus time plot $N_{Fig4} \le 0$ Suppress the figure number $N_{Fig4} > 0$ Include the figure number	
	FIG5	N_{Fig5}	F10.4	Figure number for the effective multiplication factor versus time plot $N_{Fig5} \le 0$ Suppress the figure number $N_{Fig5} > 0$ Include the figure number	
	FIG6	N_{Fig6}	F10.4	Figure number for the prompt neutron lifetime versus time plot $N_{Fig6} \le 0$ Suppress the figure number $N_{Fig6} > 0$ Include the figure number	

Table B-5. Input Requirements – Core and Thermal Hydraulic Data

Card No.	Input Variable	Symbol	Format	Description	Units
				(Card 7 is used only if m = 0, then repeat Card 7, 6 times, once for each delayed neutron group, n=1…6)	
7	**BI(N)**	β_{In}	F10.5	Input delayed neutron fraction for the n^{th} delayed neutron group	-
	ALI(N)	λ_{In}	F10.5	Input delayed neutron decay constant for the n^{th} delayed neutron group	-
8	**ZC0**	Z_c	F10.5	Initial height of the core	m
	RC	R	F10.5	Initial radius of the core	m
9	**KEFFB**	k_{eff0}	F10.7	Base line effective multiplication factor	-
10	**Q0**	Q_0	F10.4	Rated power	MW
	T0	T_0	F10.4	Inlet Temperature	^oK
				(Repeat Card 11, N_p times, once for each point in the pressure versus time table, j=1…N_p)	
11	**TI(J)**	t_{pj}	F10.5	jth time in the pressure versus time table	msec
	PT(J)	P_{pj}	F10.7	jth pressure in the pressure versus time table	MPa
				(Repeat Card 12, N_k times, once for each point in the effective multiplication factor versus pressure table i=1…N_k)	
12	**PI(I)**	p_{Ii}	F10.5	ith pressure in the effective multiplication factor versus pressure table	MPa
	KEFFI(I)	k_{effi}	F10.7	ith input effective multiplication factor in the effective multiplication factor versus pressure table	
	LPI(I)	L_{pIi}	F10.7	ith input prompt neutron lifetime in the effective multiplication factor versus pressure table	msec

B.2 SUBMITTING A QCALC1 CALCULATION

The QCALC1 code executes in a LINUX environment. LINUX commands below are in ***bold italics***. File and directory names are in **bold.**

There are ten relatively simple steps to submitting a single case QCALC1 calculation and two simple steps to obtain the output files. These are as follows.

1. Go to the proper directory, such as ***cd* home/Username/Kinetics**.
2. Type in ***vi* RUNQCALC1** – this allows you to edit the script file, **RUNQCALC1**. An example of the script files is given in Appendix B.
3. The listing of a typical single case script file is given below with a statement-by-statement explanation:

   f77 –g –LIST QCALC1.f >& error.txt - compiles the QCALC1 code and writes an error message

   cat error.txt – saves the error message so you have both a screen output and a file that can be printed

   ./a.out<INPUT*nnn*>OUTPUT*nnn* - executes the QCALC1 code, using the input file, INPUT*nnn* and writing the output file OUTPUT*nnn*

   lpr INPICQ - Plots the results for the core power versus time (usually used but Optional)

   lpr INPICT - Plots the results for the temperature versus time (Optional)

   lpr INPICP - Plots the results for the pressure versus time (Optional)

   lpr INPICR - Plots the results for the reactivity versus time (Optional)

   lpr INPICK - Plots the results for the effective multiplication factor versus time (Optional)

   lpr INPICL - Plots the results for the prompt neutron lifetime versus time (Optional)
4. Type ***i*** then change the names of both the input and output files. It is suggested that the value of the number *nnn* only be changed to keep the nomenclature consistent.
5. Type ***:w*** to save the changes.
6. Type ***:q*** to leave the script file.
7. Type ***./* RUNQCALC1** to obtain the script file for submission.
8. Hit the ***[ENTER]*** key to submit the calculation.
9. Type ***lpr* OUTSUM** to print the summary output file if desired.
10. Type ***lpr* OUTPUT*nnn*** to print the output file if desired.

B.3 OUTPUT DESCRIPTION

The QCALC1 code produces four output files:

11. The main output file
12. Summary output which contains only the pulse height parameters
13. Files that generate figures with the LINUX graphics language. Six different plots are generated including plots of the core power, core temperature, reactivity, pressure, effective multiplication factor, and prompt neutron lifetime.
14. An output file that can be imported into EXCEL data sets.

(The units of the output time are microseconds rather than seconds. The kth printed output time, t_{pk}, is calculated from the time of the kth time step, t_k, simply by converting from seconds to microseconds.)

B.4 SAMPLE INPUT DATA SETS

```
FPCR - Case # 2200 - U235 Fuel, Reflector - 20cm BeO, 1 cm WMo
2200
         2        12         5         0         1         0
         2         2         1         1         1
         3         3         3         4         3         3
1
   0.000     0.0       0.0       0.0       0.0       0.0       0.0
   1.5630    .7800
   1.0000
   1.0000   2000.00
   0.000     0.500
   0.750    50.000
   0.50     0.32733    .26214
   1.00     0.45078    .22386
   5.00     0.73928    .17388
  10.00     0.87864    .15628
  15.00     0.97473    .14223
  20.00     1.05771    .12872
  25.00     1.11874    .11938
  30.00     1.18126    .11333
  35.00     1.22873    .11206
  40.00     1.27220    .10216
  45.00     1.31513    .10365
  50.00     1.35535    .09715

FPCR - Case # 4200 - Pu239 Fuel, Reflector - 20cm BeO, 1 cm WMo
4200
         2        12         6         0         1         0
         2         2         1         1         1
         3         3         3         4         3         3
1
   0.000     0.0       0.0       0.0       0.0       0.0       0.0
   1.5630    .7800
   1.0000
   1.0000   2000.00
   0.000     0.500
   0.750    50.000
   0.50     0.31878    .21277
   1.00     0.39055    .19606
   5.00     0.65042    .15891
  10.00     0.84754    .13714
  15.00     0.99410    .13249
  20.00     1.12737    .12234
  25.00     1.22720    .11476
  30.00     1.32286    .12460
  35.00     1.41187    .10644
  40.00     1.48121    .09921
  45.00     1.55618    .09366
  50.00     1.61285    .08794
```

REPORT DOCUMENTATION PAGE

Form Approved
OMB No. 0704-0188

1. AGENCY USE ONLY *(Leave Blank)*	2. REPORT DATE	3. REPORT TYPE AND DATES COVERED
	January 2007	Contractor Report

4. TITLE AND SUBTITLE

Core Physics and Kinetics Calculations for the Fissioning Plasma Core Reactor

5. FUNDING NUMBERS

MAP-2003-V-F045
UNCLASS-0126102

6. AUTHORS

C. Butler and D. Albright

7. PERFORMING ORGANIZATION NAME(S) AND ADDRESS(ES)

Institute for Scientific Research, Inc.
320 Adams Street
P.O. Box 2720
Fairmont, WV 26555–2720

8. PERFORMING ORGANIZATION REPORT NUMBER

M–1181

9. SPONSORING/MONITORING AGENCY NAME(S) AND ADDRESS(ES)

National Aeronautics and Space Administration
Washington, DC 20546–0001

10. SPONSORING/MONITORING AGENCY REPO NUMBER

NASA/CR—2007–214724

11. SUPPLEMENTARY NOTES

Prepared for Technical Monitor: Gary Johnson

12a. DISTRIBUTION/AVAILABILITY STATEMENT

Unclassified-Unlimited
Subject Category 20
Availability: NASA CASI 301–621–0390

12b. DISTRIBUTION CODE

13. ABSTRACT *(Maximum 200 words)*

Highly efficient, compact nuclear reactors would provide high specific impulse spacecraft propulsion. This analysis and numerical simulation effort has focused on the technical feasibility issues related to the nuclear design characteristics of a novel reactor design. The Fissioning Plasma Core Reactor (FPCR) is a shockwave-driven gaseous-core nuclear reactor, which uses Magneto Hydrodynamic effects to generate electric power to be used for propulsion. The nuclear design of the system depends on two major calculations: core physics calculations and kinetics calculations. Presently, core physics calculations have concentrated on the use of the MCNP4C code. However, initial results from other codes such as COMBINE/VENTURE and SCALE4a. are also shown. Several significant modifications were made to the ISR-developed QCALC1 kinetics analysis code. These modifications include testing the state of the core materials, an improvement to the calculation of the material properties of the core, the addition of an adiabatic core temperature model and improvement of the first order reactivity correction model. The accuracy of these modifications has been verified, and the accuracy of the point-core kinetics model used by the QCALC1 code has also been validated. Previously calculated kinetics results for the FPCR were described in the ISR report, "QCALC1: A code for FPCR Kinetics Model Feasibility Analysis" dated June 1, 2002.

14. SUBJECT TERMS

nuclear reactors, gaseous core reactor, fissioning plasma core reactor, magnetohydrodynamics, core physics

15. NUMBER OF PAGES

80

16. PRICE CODE

17. SECURITY CLASSIFICATION OF REPORT	18. SECURITY CLASSIFICATION OF THIS PAGE	19. SECURITY CLASSIFICATION OF ABSTRACT	20. LIMITATION OF ABSTRACT
Unclassified	Unclassified	Unclassified	Unlimited

National Aeronautics and
Space Administration
IS20
George C. Marshall Space Flight Center
Marshall Space Flight Center, Alabama
35812